Institut für Veterinärphysiologie
der Vetsuisse-Fakultät der Universität Zürich

Direktor: Prof. Dr. Max Gassmann
Arbeitsgruppe: Prof. Dr. Thomas A. Lutz

Arbeit unter wissenschaftlicher Betreuung von
Dr. PhD Melania Osto

Human-derived antibody targeting pancreatic islet amyloid for the treatment of type 2 diabetes

Inaugural-Dissertation

zur Erlangung der Doktorwürde der
Vetsuisse-Fakultät Universität Zürich

vorgelegt von

Leoni Hugentobler

Tierärztin
von Uzwil, St. Gallen

genehmigt auf Antrag von

Prof. Dr. Thomas A. Lutz, Referent

PD Dr. PhD Eric Zini, Korreferent

Zürich 2017

Meinen Eltern Lilly und Nick,
sowie meinem Partner Oliver.

Ich danke euch von Herzen
für die grossartige Unterstützung während meiner Doktorarbeit
und dafür, dass ihr immer an mich glaubt und für mich da seid.
Ohne euch wäre ich niemals Tierärztin geworden.

Table of content

1 Zusammenfassung

Typ 2 Diabetes (T2DM) ist weltweit eine der häufigsten Erkrankungen des Menschen. Ein typisches Merkmal des T2DM sind Amyloid Ablagerungen im Pankreas, die aus dem sog. "Islet Amyloid Polypeptide" (IAPP) bestehen und deren Bildung stufenweise über die Aggregation von IAPP Monomeren zu Oligomeren und Fibrillen abläuft. Toxische IAPP Oligomere sind wahrscheinlich für Funktionsstörungen der β-Zellen und letztlich deren Zelltod verantwortlich. Keine der momentan verfügbaren T2DM-Behandlungen richtet sich gegen die Aggregation von IAPP. Ein Antikörper (NI-203.26C11), welcher humane IAPP Aggregate bindet, wurde *in vitro* und *in vivo* identifiziert, geklont und charakterisiert. Da IAPP von Ratten nicht amyloidogen ist, wurden transgene Ratten verwendet, die das humane IAPP Gen (hIAPP, RIPHAT Ratten) exprimieren. NI-203.26C11 verbesserte die Glukose Toleranz sowie die β-Zell Funktion, erhöhte die Insulin Sekretion, reduzierte die Nüchternglukose und normalisierte die Gewichtszunahme bei den RIPHAT Ratten im Vergleich zu Kontrolltieren. In einer Dosis-Wirkungs-Studie wurden die drei getesteten Dosierungen (1, 3, 10 mg/kg) als sicher und wirksam eingestuft. Interessanterweise zeigten 1 mg/kg und 10 mg/kg eine bessere Wirkung als 3 mg/kg bezüglich der Glukose Toleranz und der Erhöhung der Insulin Sekretion. Die tiefere Dosierung normalisierte sogar die Gewichtszunahme. Folglich stellt die passive Immunisierung eine vielversprechende Strategie in der Behandlung von T2DM dar.

2 Summary

Type 2 diabetes (T2DM) is one of the most important public health challenges in humans. One of the hallmarks of T2DM is the deposition of islet amyloid derived from islet amyloid polypeptide (IAPP) in pancreatic islets. Amyloidogenesis involves the stepwise aggregation of IAPP monomers into oligomers, fibrils and, ultimately, mature amyloid deposits. The small toxic IAPP oligomers seem to cause β-cell failure and death. None of the available treatments against T2DM counteracts the aggregation of IAPP and the subsequent loss of pancreatic β-cells. A human-derived antibody NI-203.26C11, which targets human IAPP aggregates was identified, cloned and characterized *in vitro* and *in vivo*. Because rat IAPP is not amyloidogenic, transgenic rats with the human IAPP gene (hIAPP, RIPHAT rats) were used. NI-203.26C11 significantly improved glucose tolerance and β-cell function, increased insulin secretion and pancreatic insulin content, reduced fasting glucose and normalized body weight in NI-203.26C11-treated RIPHAT rats compared to controls. In a dose-response study, three different doses of NI-203.26C11 (1, 3, 10 mg/kg) were found to be safe and effective in slowing the progression of T2DM. Interestingly, 1 mg/kg and 10 mg/kg were generally more effective than 3 mg/kg in improving glucose tolerance and insulin secretion. The lower dose even normalized body weight gain. As conclusion, passive immunization targeting IAPP aggregates is a very promising approach to treat T2DM.

3 Introduction

3.1 Epidemiology and risk factors of type 2 diabetes mellitus (T2DM)

Diabetes mellitus is known to be one of the most relevant public health challenges all over the world. The number of people with diabetes mellitus has more than doubled over the past three decades [1]. Global estimates showed a prevalence of diabetes in 285 million people in 2010 [2], 90% of whom had T2DM [3]. Newer studies indicated an increased worldwide prevalence of diabetes with 415 million people in 2015 and an expected rise to 642 million people by 2040 [4].

T2DM is a complex illness and depends on interactions between genetic and epigenetic predispositions and risk factors such as obesity, physical inactivity, history of smoking, being male and hypertension. Overweight and obesity represent the most important risk factors for T2DM with the high majority (80-85%) of diabetes cases arising from overweight or obese individuals [5].

3.2 Pathogenesis of T2DM

The main features of T2DM are insulin resistance and β-cell failure which results from reduced β-cell function and/or β-cell mass and leads to defective insulin secretion. Inadequate insulin secretion causes hyperglycemia whose micro- and macrovascular consequences are atherosclerosis, retinopathy, nephropathy and neuropathy [6], [7], [8]. Mechanisms leading to β-cell failure in T2DM include gluco- and lipotoxicity as well as the development of islet amyloid deposits caused by islet amyloid polypeptide (IAPP), which is also called amylin. Due to the presence of amyloid deposits in T2DM patients, the disease is considered a protein misfolding pathology, and in that sense similar to at least 30 other disorders, mostly neurodegenerative disorders such as e.g. Alzheimer's, Parkinson's and Huntington's chorea [7], [9], [10].

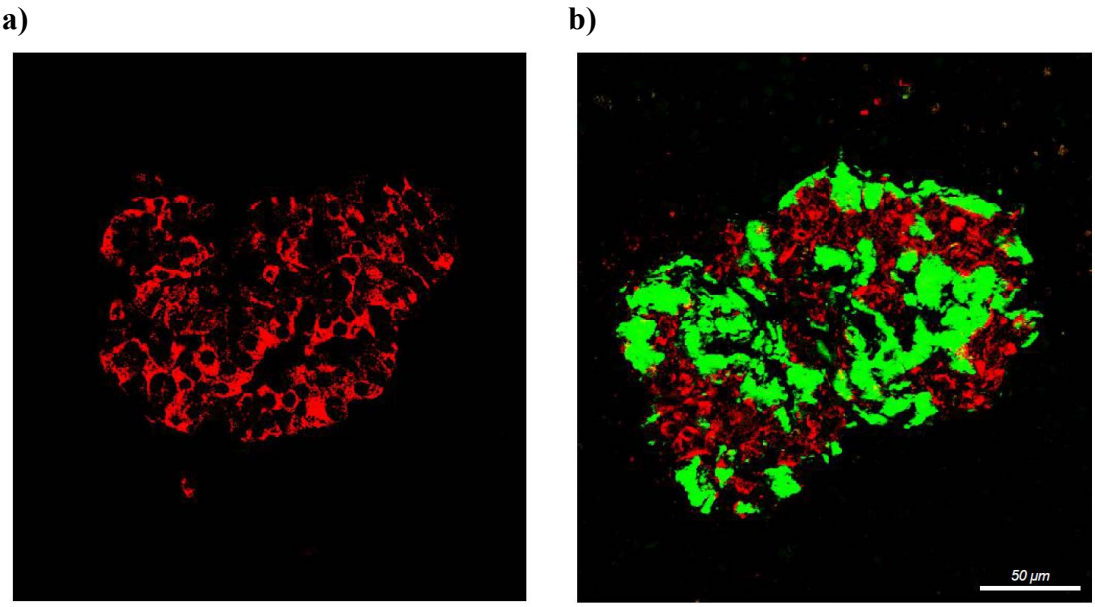

Figure 1: Immunohistochemical analysis of pancreatic islets of a healthy person **(a)** and a person suffering from T2DM **(b)**. Representative fluorescent images of islets stained for insulin (red) and ThioS-positive amyloid (green). Healthy person **(a)** shows a normal amount of insulin in the β-cells of pancreatic islet. T2DM person **(b)** shows a decreased amount of insulin with a large amount of amyloid deposits. Scale bar: 50 µm (Images from Neurimmune AG, Schlieren).

3.2.1 Insulin secretion

In normally functioning β-cells, insulin secretion occurs in two phases. The first phase arises rapidly after blood glucose increases, lasts only a few minutes and releases a readily releasable pool (RRP) of insulin secretory granules. The second phase is characterized by a slow and sustained release of new insulin granules mobilized from the reserve pool (RP) [11]. Different complex pathways control this glucose-stimulated insulin secretion. In the "triggered pathway" during the first phase, the uptake of glucose into the β-cells induces the release of insulin by the secretory granules via the formation of mitochondrial ATP production followed by closure of ATP-sensitive K^+-channels and by β-cell depolarization [12], [11], [13], [14]. To support the "triggered pathway" after glucose uptake, the still poorly understood "metabolic amplifying pathway" generates down-stream metabolites that amplify insulin secretion especially in the second phase of insulin release [11], [15], [14]. Insulin secretion is activated not only by glucose but also by hormones (e.g. the incretins glucagon-like peptide-1 (GLP-

1) and glucose-dependent insulinotropic polypeptide (GIP)) and neurotransmitters such as acetylcholine in so-called “neurohormonal pathways” [11].

3.2.2 Insulin action

Insulin binds to the insulin receptor on the surface of many tissues and acts as anabolic hormone. It is necessary for the development and growth of tissues and the regulation of glucose-homeostasis by glucose-uptake in muscle and adipose tissue and a decreased glucose release by the liver [13], [16]. Insulin action is controlled by various mechanisms, amongst others by circulating hormones (e.g. glucagon), cytokines, non-esterified (free) fatty acids (NEFA) and glycerol released by adipose tissue, especially by large adipocytes in visceral or deep subcutaneous fat depots [12].

3.2.3 Insulin resistance

As often seen in obese individuals, an enhanced release of NEFA and inflammatory cytokines like tumor necrosis factor-α (TNFα) and interleukin-6 (IL-6) affects the insulin-signaling cascade and leads to insulin resistance with impaired or failed activation of the insulin receptor of peripheral tissues [12], [13]. The ability for glucose-uptake in muscle and adipose tissue is reduced whereas the liver proceeds with gluconeogenesis. This condition results in hyperglycemia [17].

3.2.4 β-cell dysfunction in obesity and T2DM

In the presence of insulin resistance, insulin secretion is enhanced to sustain normal blood glucose levels which may lead to an increase in β-cell mass. While this compensatory mechanism is sufficient to maintain the homeostasis of glucose levels in many obese individuals, the β-cell capacity may be exhausted in particular in people who are genetically at risk of T2DM with the consequent progressive increase in circulating levels of glucose [6].

The higher oxidative metabolism of glucose induced by hyperglycemic states results in an increased production of reactive oxygen species (ROS), leading to endoplasmic reticulum (ER) stress and mitochondrial dysfunction, and ultimately to β-cell apoptosis; this sequence of events is s also known as gluco-toxicity [9].

In obese individuals, dyslipidemia with enhanced NEFA and disturbed lipoprotein levels can occur [9]. Long-term exposure to high NEFA concentrations also induces oxidative stress in β-cells and suppresses insulin secretion (lipo-toxicity) [14]. The concentrations of pro-apoptotic low density-lipoproteins (LDL) and very low density-lipoproteins (VLDL) are increased and contribute to progressive β-cell failure, while high density-lipoproteins (HDL), having a protective effect by inhibiting β-cell apoptosis, are decreased [9].

In the presence of hyperglycemia, mitochondrial β-oxidation of fatty acids is impaired and the following accumulation and esterification of the remaining fatty acids leads to harmful high amounts of long chain acyl-CoA. Although the exact mechanism of this so-called glucose induced lipo-toxicity or gluco-lipo-toxicity is not completely understood, increased amounts of long chain acyl-CoA during hyperglycemia lead to aggravated β-cell function and decreased insulin secretion [9], [18].

3.3 Islet amyloid polypeptide (IAPP) or amylin

IAPP is stored as 89-amino acid (aa) preproIAPP together with insulin in the secretory granules of the β-cells. IAPP is co-secreted with insulin in a ratio of ca. 1:100 (IAPP:Insulin). In a first step, a 22-aa signal sequence is cleaved off in the endoplasmic reticulum. The remaining 67-aa precursor proIAPP undergoes processing by the two endoproteases, i.e. prohormone convertase 2 (PC2) and prohormone convertase 1/3 (PC1/3) and the carboxypeptidase E (CPE) to cleave off two flanking peptides at the C- and N- terminal ends in the trans Golgi network or secretory granules, respectively. Insulin is cleaved from proinsulin to the mature insulin by the same enzymes. A disulfide bond between cysteine residues 2 and 7 and a C-terminal amide (Tyr37) are constructed via posttranslational modification to yield the biologically active 37-aa peptide IAPP, which is then co-secreted with insulin [19] ,[20], [21], [22].

The IAPP amino acid sequence is closely related to calcitonin-gene related peptide (CGRP), calcitonin, adrenomedullin and adrenomedullin 2 [23], [24]. IAPP is a satiating hormone which decreases food intake, inhibits gastric emptying and also the postprandial glucagon release to lower blood glucose levels [25], [26], [27]. IAPP also acts as an adiposity signal and increases energy expenditure [27], [28]. IAPP's effects occur via different amylin receptors, belonging to a large superfamily of cell surface G protein-coupled receptors and being closely related to calcitonin receptors. These

receptors contain one of three different RAMPs (receptor activity modifying protein), and with different slice variants of the calcitonin core receptor, several variable amylin receptor subtypes are formed [24], [29], [30]. Hormonal IAPP acts via the area postrema (AP) to induce the above mentioned effects [27].

3.3.1 Differences between species

Non-human primates and cats are the only non-human species showing pancreatic islet amyloid deposits and being prone to developing a form of T2DM which mimics the human features. The primary structure of IAPP is highly conserved among species, besides differences in the amino acid residues 20-29 which do not seem to be critical for the hormonal action of IAPP [31], [32], [33], [34]. IAPP from primates and cats easily aggregates by forming β-sheet structures. In contrast, in mice and rats, three proline residues within the region 20-29 were shown to act as β-sheet breakers [35] and therefore, rodents, even though they synthesize and secrete IAPP, do not exhibit islet amyloid or suffer from a T2DM- like syndrome [36], [37], [38].

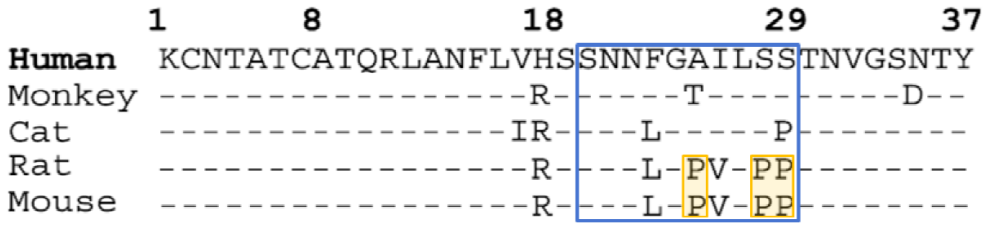

Figure 2: Primary structure (aa1-37) of IAPP in several species: The amyloidogenic region contains aa- residues 20-29 (blue). Due to three proline residues (orange) in this region of IAPP in rats and mice, these species are not prone to developing islet amyloid and a T2DM-like syndrome (modified by E. Jaikaran et al., 2001).

3.4 Pancreatic islet amyloid

Pancreatic islet amyloid was first described in 1901 as homogenous material that stains with eosin and was originally called hyaline material [39]. IAPP-derived amyloid deposits can be found in over 90% of all human patients suffering from T2DM, but also in some mostly elderly people without diabetes [37]. These findings in healthy individuals gave rise to the question whether and how islet amyloid is related to the

pathogenesis of T2DM. There is strong evidence that the formation of toxic oligomers derived from amyloidogenic IAPP causes β-cell dysfunction and apoptosis leading to impaired insulin secretion, and plays an important role in the pathogenesis of T2DM [7], [10].

Mature amyloid deposits, visible by light microscopy, may impair the cell-to-cell contact through connexin-36 gap junction channels by occupying the space between β-cells and thus lead to reduced transfer of insulin and nutrients between the cells [21], [37]. However, the main cytotoxic species of IAPP are intracellularly formed small oligomers causing membrane disruption and leakage. These small oligomers are only visibly by electron microscopy. Because rodent IAPP is not amyloidogenic, mice and rats transgenic for human IAPP (hIAPP) have been generated to study underlying mechanisms. It has e.g. been observed that homozygous hIAPP transgenic mice, which develop diabetes quite early in life (10 weeks of age) due to high β-cell loss, did not show any extracellular islet deposits at this stage. Hence, the "amyloid hypothesis" that suggests that mature amyloid deposits cause cytotoxicity, had to be given up and the pathophysiology is probably explained better by the so-called "toxic oligomer hypothesis". Nonetheless, since large fibrils achieve a stationary phase with a balance between assembly and dismantling of oligomers, it is suggested that large amyloid deposits may represent a reserve for small toxic oligomers [6], [10], [40], [41]. However, the mechanisms causing β-cell death are still not fully understood [42].

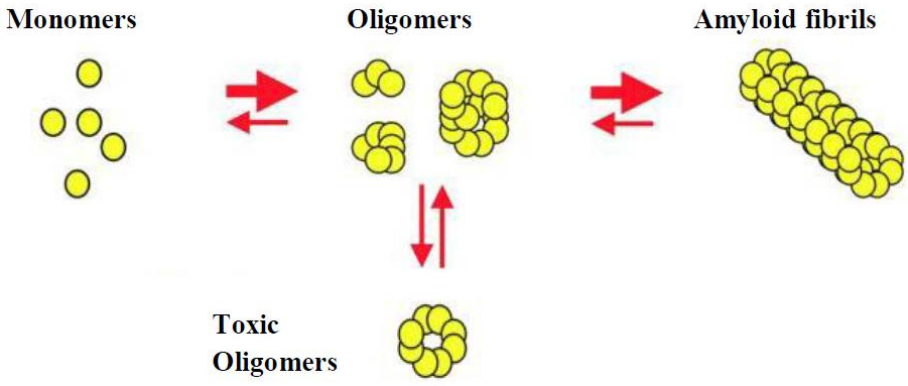

Figure 3: Schematic image of formation of IAPP oligomers and amyloid fibrils originating from IAPP monomers. Oligomers can lead to toxic oligomers (modified by L. Haataja et al., 2008).

3.4.1 Islet amyloid formation

Besides the harmful effects of high glucose and disturbed lipid levels (see 3.2.4), one of the main causes of β-cell exhaustion is the enhanced rate of apoptosis in β-cells due to increased endoplasmic reticulum (ER) stress induced by high levels of misfolded hIAPP, finally resulting in the formation of visible islet amyloid deposits [6], [43].

Important factors leading to amyloid formation are environmental changes, abnormal pro-hormone processing and advanced glycation of hIAPP end products and insulin. Since insulin and hIAPP are co-secreted, an abnormal increase of local intracellular hIAPP is associated to the increase in insulin secretion caused by insulin resistance [37], [44]. It is known that insulin and a low pH in the secretory granules have a stabilizing effect on hIAPP, preventing the fibril formation [10]. Proinsulin, which is often increased in the secretory granules of the β-cells during the process of T2DM, has not such a preventing effect, leading to a higher rate of intracellular hIAPP oligomer formation. Additionally, mutations in the hIAPP gene, such as the S20G mutation (heterozygous substitution of hIAPP at position 20 of a serine residue for a glycine), may lead to a more amyloidogenic version of hIAPP and, therefore, cause enhanced amyloid formation [37], [44], [45].

A predicted model of the secondary structure of hIAPP monomers consists of three antiparallel β-sheets composed of three amyloidogenic regions, built up by a first β-turn at asparagine31 and a second one at serine20, leading to an intramolecular β-sheet stabilized through several hydrogen bonds [46]. Later, it was assumed that the monomers form two β-strands, connected by a loop containing the amyloidogenic region 20-29, linked by several hydrogen bonds [42]. The aggregation of misfolded monomers leads to the formation of oligomers with a tertiary structure of crossed β-sheets [21], [38]. Gurlo and coworkers demonstrated that toxic oligomers are formed in the secretory pathway and escape into the cytosol by causing direct membrane damage [47]. While it is still not clear, if toxic oligomers and amyloid fibrils result from the same aggregation-pathway, it seems that both of them have an intracellular origin [42].

“Nucleation-dependent fibrillation” represents the prevailing model of amyloid formation not only in T2DM but also in other protein-misfolding diseases such as e.g. Alzheimer’s, Parkinson’s and Huntington’s chorea. The “nucleation-dependent fibrillation” takes place in three successive phases: the first or so-called lag phase with nucleus formation out of mono- and oligomers acting as template, but no fibrillar growing, the second exponential growth phase with accelerated fibrillation due to

accelerated adhesion of monomers and finally, the stationary phase with no additional fibrillar growth based on a balance between build-up and decomposition of the amyloid fibrils [10], [48].

IAPP amyloid deposits could also be found in kidneys, the temporal-lobe gray matter of the brain and in blood vessels and IAPP oligomers in the heart of T2DM patients [10]. Pancreatic amyloid deposits in humans, monkeys and cats start as small fibrils close to islet capillaries in single islets, spread to almost all islets (increasing islet prevalence) and finally lead to an increased amount of amyloid deposits per islet [37]. In 2011, Jurgens and coworkers demonstrated that in T2DM, the β-cell mass decrease due to apoptosis is strongly related to increasing amounts of islet amyloid [7].

3.4.2 β-cell dysfunction due to islet amyloid

3.4.2.1 Apoptosis

In T2DM, toxic intracellular small oligomers induce β-cell apoptosis through the intrinsic pathway mostly by initiating ER stress, mitochondrial dysfunction, oxygen stress and inflammation, while the extrinsic pathway is activated by extracellular receptor-binding due to inflammation or direct cell membrane disruption [6], [38], [49]. It seems that hIAPP fibrils, rather than toxic oligomers, cause direct membrane damage [22].

3.4.2.2 Mechanisms activating the intrinsic pathway

The normal function of the endoplasmic reticulum (ER) is to synthetize and fold secretory proteins and to transfer them into the Golgi and secretory vesicles. Under normal conditions, the unfolded protein response (UPR), high Ca^{2+} concentrations and also an oxidative environment in the ER prevent misfolding of secretory proteins. The UPR ensures the ER function by activating several mechanisms leading to decreased translation of main ER client proteins. Furthermore, the UPR provides increased amounts of chaperones, necessary for the prevention of misfolding, and other proteins responsible for the clearance of un- and misfolded ER proteins. In T2DM, insulin resistance leads to an increased synthesis and secretion of insulin and IAPP, causing an overload in the ER. This leads to a highly increased burden for the UPR and any additional charges can easily lead to an imbalance of this protective system; finally, ER-

stress induced apoptosis may occur. Misfolded hIAPP oligomers may then lead to membrane disruption by causing nonselective ion channel activity and Ca^{2+} leakage of the ER, followed by mitochondrial membrane leakage of cytochrome c and activation of several caspases, protein kinases involved in the initiation of apoptosis. Additionally, Ca^{2+} leakage through toxic hIAPP oligomers activates ER associated calpain with the ability to induce caspase-independent apoptosis [6], [47].

Besides acting as nonselective ion channels, toxic hIAPP oligomers can directly disrupt the membranes of the secretory pathway in β-cells. Subsequently, toxic hIAPP oligomers in the cytosol cause direct membrane-damage of cytosolic cell organelles such as mitochondria, finally leading to mitochondrial dysfunction induced apoptosis [47]. Additionally, hIAPP oligomers can lead to instable mitochondrial membrane potential, causing high amounts of harmful reactive oxygen species (ROS) [10].

Especially in long living cells such as β-cells, there are three characterized mechanisms to remove misfolded or otherwise damaged proteins: the ubiquitin proteasome system (UPS), autophagy and aggresome formation. The UPS operates by marking abnormal proteins with ubiquitin chains. This leads to entering the proteolytic proteasome after removing ubiquitin chains by several enzymes. In β-cells, the most common deubiquinating enzyme is the ubiquitin carboxyl-terminal hydrolase L1 (UCH-L1). It seems that enhanced amounts of hIAPP decrease the expression of UCH-L1 in β-cells by unknown mechanisms, causing deterioration in the UPS, leading to accumulation of ubiquinated proteins and cytotoxicity.

Autophagosomes are membrane-bound vesicles, enclosing damaged proteins or other cell structures, conveying them to the lysosome where proteolysis takes place [10]. It is suggested that hIAPP oligomers impair lysosomal proteolysis, leading to high concentrations of hIAPP aggregates and cell death. The so-called aggresome is the designation of cytosolic inclusions at the microtubule organizing center, enclosing escaped misfolded proteins to ensure their degradation by the UPS or autophagy. However, if the function of the UPS and autophagosome system is impaired, aggresomes cannot be abolished, leading to β-cell apoptosis through different above described mechanisms [10].

3.4.2.3 Mechanisms activating the extrinsic pathway

Amyloid deposits are known to cause inflammation in affected islets [38]. Immune cell infiltration seems to take place in all patients suffering from T2DM [8]. Phagocytosed aggregates may lead to inflammasome-activation in macrophages, a molecular multi-protein complex causing the release of inflammatory cytokines such as IL-1β and IL6 [10], [38]. Increased secretion of these pro-inflammatory cytokines seems to activate the extrinsic pathway by ligand binding [50]. Additionally, direct extracellular binding of toxic hIAPP to the "death receptor" FAS also activates the extrinsic pathway, causing apoptosis by the activation of caspase 3 [38].

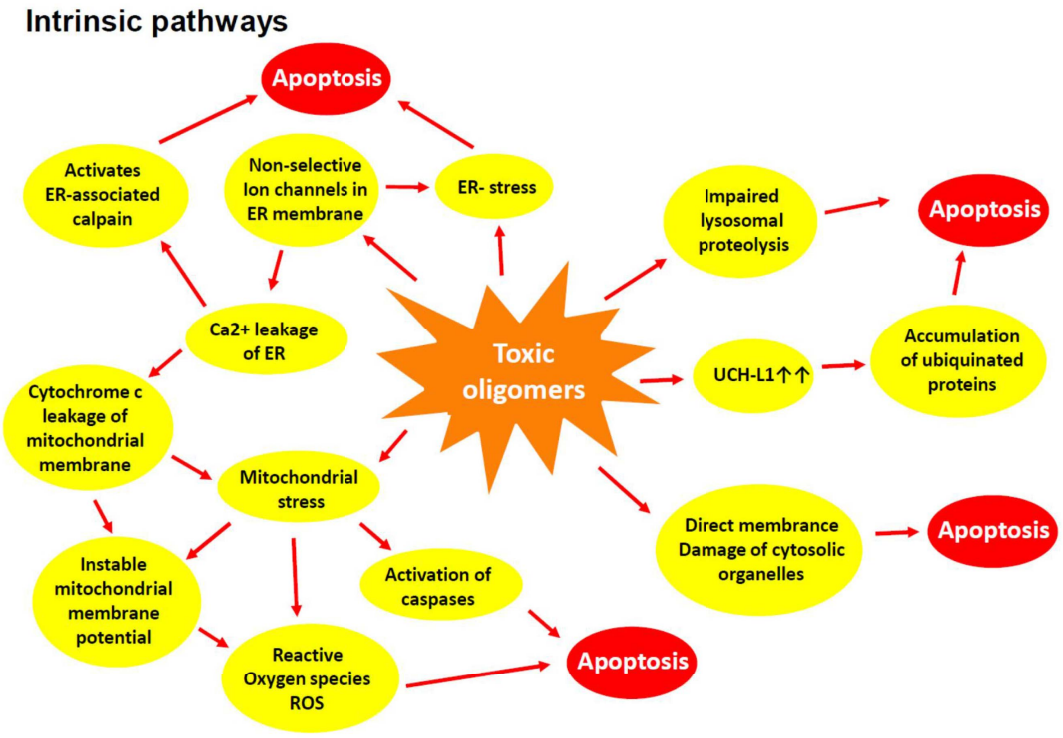

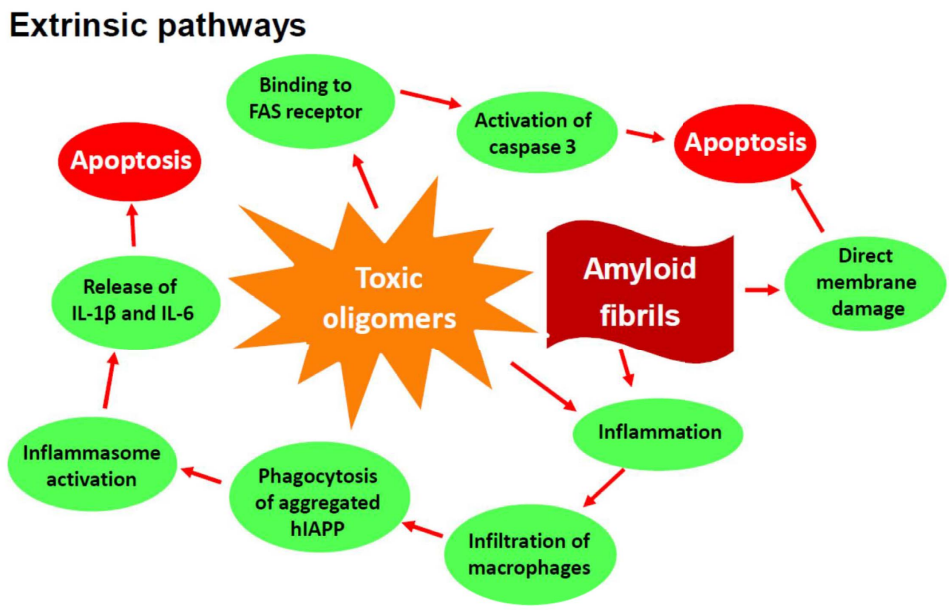

Figure 4: Intrinsic and extrinsic pathways of apoptosis in β-cells caused by toxic oligomers or amyloid fibrils. ER= endoplasmic reticulum, UCH-L1= ubiquitin carboxyl-terminal hydrolase L1, IL-1β= Interleukin-1β, IL-6= Interleukin-6.

To finally understand the complicated nature of islet amyloid and its effect on β-cell survival, it is important to appreciate that all the above described pathological mechanisms, leading to this complex disease pattern, take place in parallel and interact with each other in various ways. Whether islet amyloid is a cause of T2DM or a consequence, leading to further loss of β-cells and hence contributing to the severity of the disease, still needs further investigation.

3.5 Rodent models of T2DM

Diabetes not only negatively influences the quality of life of affected people, but also causes immense health care costs. In 2014, it has been estimated that the worldwide cost of T2DM was at least 612 billion USD, and Europe, North America and the Caribbean Region caused about 69% of the above mentioned costs [51]. The fact that T2DM is increasingly seen in young adults [52], with a particularly high risk of cardiovascular diseases [53], leads to the obvious conclusion, that there is an urgent need of strategies to prevent the development and to improve the treatment of T2DM [54], [55]. T2DM in humans is a slowly progressive disease, characterized by defective insulin secretion due to β-cell dysfunction or loss of β-cell mass, insulin resistance and deposition of islet

amyloid derived from hIAPP. It usually takes years for the full clinical picture including micro- and macrovascular complications to develop [6], [54], [55]. Therefore, the use of animal models which show a much faster development of diabetes, its symptoms and complications represents a logical and efficient strategy in research. So far, there is no rodent model comprehensive of all characteristics of T2DM, including the same pathogenesis, symptoms and complications. However, there are several rodent models mimicking at least some aspects of T2DM [55], [56], [57]. An example of a rodent model that mimics the pathophysiology of obesity and insulin resistance, leading to elevated blood glucose levels, represents the diet induced obesity (DIO) mouse, a C57BL/6 mouse developing a diabetic syndrome when fed with high fat diet [58], [59].

3.5.1 hIAPP transgenic models

Since rodent IAPP is not amyloidogenic, the development of transgenic mice and rats expressing the hIAPP was necessary to study this particular aspect of the T2DM pathophysiology [59]. These models helped to study the pathophysiology of islet amyloid and the effectiveness of anti-amyloid treatment in rodents. Due to the human transgene in these animals, the study of amyloid deposits in T2DM became possible [54]. Spontaneously developing diabetes was observed in transgenic mice homozygous for hIAPP (h-IAPP(homozygous):FVB/N) [60], while hemizygous transgenic hIAPP mice (h-IAPP(hemizygous):C57BL76J) did not become diabetic [61]. Actually, in heterozygous mice, several strategies are needed to increase the burden of the transgene to initiate a diabetic phenotype [54]. The administration of growth hormone or dexamethasone (h-IAPP(hemizygous):FVB/N) [62], high fat feeding (h-IAPP(hemizygous):C57/6xDBA) [63], and crossbreeding onto an obese background such as Avy/Agouti (h-IAPP(hemizygous):A^{vy}/A) or $Lep^{ob/ob}$ (h-IAPP(hemizygous): ob/+) were described to provoke a diabetic phenotype with impaired glucose tolerance, amyloid deposits and hyperglycemia [64], [65].

Similar to the mouse models, the HIP rat (hIAPP) or RIPHAT rat (rat insulin II promoter human IAPP transgenic rat) is a transgenic rat model expressing hIAPP, which was generated by Butler and colleagues in 2004 to overcome the limitations often seen in mice [66]. A transgene construct with a cDNA sequence coding for the human IAPP and the rat insulin II promoter was generated and microinjected to fertilized Sprague Dawley rat eggs. The hemizygous line, exhibiting a midlife onset of diabetes

due to hIAPP expression in β-cells and representing the usual onset of the disease in humans, was identified. Because males are more prone to diabetes than females, only male rats of this line were selected (HIP or RIPHAT rats, see table 1 for characteristics). Homozygous rats developed an early onset of diabetes without visible amyloid deposits [66].

Table 1: Comparison between Sprague Dawley rats and hemizygous RIPHAT rats (modified by Butler et al., 2004).

Criteria	Wild type control rat (Sprague Dawley: SD)	RIPHAT rat (CD:SD-Tg(ins2-IAPP)Soel)
Bodyweight (BW)	Normal BW of Sprague Dawley rats (Charles River Laboratories)	20% lower than wild type rats after 5 months of age
β- cell mass	Increased by 60% from 5 to 18 months of age	Decreased by 90 % from 5 to 18 months of age, with a 60% decrease at the onset of diabetes
β-cell replication and apoptosis	Constant rate of replication and apoptosis from 5 to 18 months of age	Increased rate of replication and apoptosis from 5 to 18 months of age, replication not able to compensate for increased apoptosis, leading to loss of β- cell mass
Islet amyloid	No islet amyloid at any stage	Islet amyloid present at 2 months of age, increasing and reaching a plateau at 10 months of age
Phenotype	No impaired fasting glucose and no onset of diabetes at any stage	Impaired fasting glucose at 5 months of age, onset of diabetes between 5 and 10 months of age

3.6 Anti-amyloid treatment

Management of T2DM usually involves lifestyle changes such as diet and exercise to lose body weight, leading to improved tissue insulin sensitivity. It also includes treatment with a large number of anti-diabetic drugs to lower the high blood glucose levels and, if necessary, antihypertensive and anti-platelet medications against diabetes associated complications [12], [67]. No approved drug, however, is available to inhibit IAPP aggregation and the subconsequent impairment in β-cell function [10].

3.6.1 Aromatic organic compounds

In 1994, Congo Red was shown to inhibit hIAPP amyloid fibril toxicity but did not prevent the formation of hIAPP fibrils *in vitro* [68]. However, Aitken and coworkers published contradictory results in 2003, demonstrating the ability of Congo Red to not only inhibit the hIAPP toxicity and fibril formation but also to reduce hIAPP amyloid content *in vitro* [69]. Rifampicin and its analogues, p-benzoquinone and hydroquinone, were shown to inhibit the toxicity of aggregated hIAPP peptides without preventing the hIAPP fibril formation *in vitro*. This inhibitory effect on hIAPP aggregate toxicity is caused by the binding to hIAPP fibrils and by preventing their contact to the cell-surfaces [70]. On the other hand, Meier and coworkers demonstrated in 2006 that rifampicin does prevent the formation of mature hIAPP fibrils but not the formation of toxic hIAPP oligomers *in vitro* [71]. Therefore, the administration of rifampicin did not protect intracellularly hIAPP expressing RIN cells, nor β-cells of isolated pancreatic rat islets of RIPHAT rats from hIAPP toxicity caused by toxic hIAPP oligomers. In fact, the addition of rifampicin to the above mentioned *in vitro* and *ex vivo* cells rather increased the cell-toxicity of toxic hIAPP oligomers. A possible explanation might be that the inhibition of fibril formation by rifampicin prevented oligomers to be transferred into potentially less toxic large fibrils and thus lead to a higher amount of toxic hIAPP oligomers. Hence, the administration of rifampicin or related structures appears to be unsuitable in preventing T2DM [71].

3.6.2 Unmodified short peptides

Short peptides derived from hIAPP amyloidogenic regions were designed and tested *in vitro* for their effects on the fibrillogenesis of the full-length peptide (see also figure 2). Peptides containing the hIAPP sequences 20-25 and 24-29 from the amyloidogenic region 20-29 (SNNFGAILSS) of hIAPP were shown to inhibit β-sheet formation and amyloid aggregation, while the peptide 22-27 (NFGAIL) rather increased the ability of hIAPP to form insoluble fibrils [72], [73]. The hIAPP residues 13-18 (ANFLVH) from a second fibrillogenic hIAPP region [74] were shown to be potent amyloid aggregation inhibitors *in vitro* [75]. Recently, the anti-amyloid efficacy of the residues 13-18 (ANFLVH) of hIAPP have been tested *in vivo* by using a hIAPP transgenic mouse model, leading to improved glucose tolerance by reduced islet cell apoptosis and

preservation of β-cell area in transgenic mice treated with ANFLVH compared to transgenic control mice [76].

3.6.3 Modified short peptides

Another peptide-based strategy was rested upon the use of structure-based non-amyloidogenic derivatives of the hIAPP peptide. Double N-methylation of the hIAPP fibrillogenic region 22-27 [77] increased the binding-affinity of derivatives to full-length hIAPP, prevented the aggregation of fibrils into amyloid and decreased β-cell apoptosis [78]. The N-methylated derivative was used to generate a full-length molecular mimic of hIAPP called IAPP-GI [79] that was shown to inhibit the amyloid aggregation and cytotoxicity of unmodified hIAPP *in vitro* [80]. Another group demonstrated that a point-mutation of isoleucine at position 26 to a proline residue transformed the natural hIAPP sequence into a potent amyloid aggregation inhibitor [81].

An all-D-amino-acid substituent of hIAPP segment 22-27 (NFGAIL) revealed to be another successful peptide-based approach to inhibit amyloid formation [82]. Whereas most of these approaches targeted amyloid fibrils [77], [78], [80], [81], other studies demonstrated that two pentapeptides derived from the incorporation of non-natural amino acid (α,β-dehydrophenylalanin) into the amyloidogenic core region of hIAPP22-27 were capable of binding monomeric forms of hIAPP and to decrease the formation of hIAPP oligomers [83]. Because of the increasing evidence for oligomers to be more toxic than mature fibrils [6], [84], inhibition of hIAPP aggregation at the earliest stage before oligomers are formed, is thought to be the most promising strategy [83].

3.6.4 Flavonoids and other strategies

Flavonoids such as flavonol (-)-epigallocatechin 3-gallate (EGCG) [85], [86] and the hydroxyflavone Morin hydrate [87] have been shown to not only inhibit amyloid fibrillation by binding to hIAPP monomers, intermediates and fibrils, but even to disaggregate hIAPP amyloid fibrils *in vitro*.

Recently, several additional strategies to prevent hIAPP amyloid formation have been under investigation. One *in vitro* approach took advantage from the inhibitory effect of Copper ions [Cu(II)] on hIAPP aggregation [88]. Another research group has examined the application of a polymeric nanoparticle, the generation-3 OH-terminated poly

(amidoamine) dendrimer, to bind to the amyloidogenic hIAPP residues 22-29 and therefore, to inhibit hIAPP amyloid aggregation [89]. Last, the heat shock protein Hsp72 (HSPA1A) showed inhibitory effects against hIAPP aggregation and cell-toxicity *in vitro*. Additionally, Hsp72 enhanced h-proIAPP solubility *in vivo* in a novel transgenic h-proIAPP C. elegans model [90].

3.6.5 Immunotherapy

Similar to T2DM, Alzheimer's disease (AD) is also a member of the so-called protein-misfolding or amyloid diseases that are due to aggregating proteins leading to oligomers and amyloid fibrils with harmful effects such as oxidative stress and inflammation, finally causing loss of neurons or β-cells, respectively [10], [91]. While islet amyloid in T2DM is built up by IAPP, the aggregating protein in AD is amyloid-β protein (Aβ), leading to extracellular neuritic plaques [92]. The most widely developed and promising approach to target Aβ in AD is the use of passive immunotherapy. Several phase III clinical trials for antibodies, such as Crenezumab [92] or Aducanumab from Neurimmune Holding AG (Schlieren, Switzerland), are still ongoing [93] and some phase III clinical trials, e.g. for the antibody Solanezumab, are already conducted [94]. Considering these approaches to treat AD, it seems obvious that amyloid-directed immunotherapy may also be an attractive approach to target islet amyloid deposits in T2DM.

Several research groups investigated the use of an immunotherapeutic approach to treat T2DM. Bram and coworkers detected specific antibodies from human diabetic donors that were able to bind toxic oligomers and to decrease their cytotoxicity *in vitro* [84]. Their work not only confirmed the toxic oligomer hypothesis (see 3.4, [6]) by identifying IAPP soluble oligomers to be the most cytotoxic forms during the process of T2DM, but also supported the idea of using antibodies to target IAPP for the treatment of T2DM. To design anti-amyloid domain antibodies specific for IAPP in T2DM and Aβ in AD, Lee and coworkers used a motif-grafting approach *in vitro* by grafting amyloidogenic peptide segments of IAPP and Aβ into complementarity-determining regions of single domain antibodies. However, these specific anti-IAPP domain antibodies have not yet been tested *in vivo* [95].

Krishnamurthy and coworkers used hemizygous hIAPP transgenic mice on a mixed DBA/2-C57Bl-6 background to investigate the feasibility of an active

immunotherapeutic approach to target islet amyloid aggregates by injecting full-length hIAPP or a hIAPP derivative containing the amino acids 7-19 (IAPP7-19) [96]. The modest antibody response of monthly vaccination between 2 and 14 months of age against full-length hIAPP in the IAPP7-19 derivative study seemed to be sufficient to bind toxic soluble oligomers. The very high anti full-length antibody response generated in the full-length hIAPP study appeared to lead to a negative effect on glucose regulation. Since it may be quite difficult to control a specific level of antibody response in different individuals, it seems that passive immunization with IAPP targeting antibodies might be preferable to active immunization strategies [96].

3.7 Preliminary data

Preliminary studies were conducted to test the therapeutic efficacy of a passive immunization with high affinity human-derived antibodies targeting pathologically misfolded forms of hIAPP in transgenic rodent models of T2DM expressing hIAPP. Because the toxic effect of amyloid fibrils may be due to small oligomers within the cells, before extracellular amyloid is visible, lead antibody candidates that target misfolded hIAPP have been identified, cloned and reproduced.

Identified antibodies were validated *in vitro* for their affinity and selectivity to pathological hIAPP oligomers and fibrils in pancreatic tissue of human diabetic subjects. The NI-203.26C11 antibody showed very high selectivity for pathological hIAPP and no binding to the native conformation of physiological monomeric hIAPP in healthy subjects. Thus, NI-203.26C11 was selected for validation *in vivo* in transgenic models expressing hIAPP. All data were generated in collaboration with Neurimmune AG, Schlieren.

3.7.1 Mouse study

In FVB/N-Tg(Ins2-IAPP)RHFSoel/J mice, the chronic administration of the antibody NI-203.26C11 was well tolerated and safe. However, the phenotype of the "RIPHAT" homozygous mice was very severe and diabetes progressed rapidly. Spontaneous death was observed during the experimental time in both NI-203.26C11- or PBS-treated homozygous groups. The immunotherapy did not improve glucose control, glucose tolerance and insulin secretion nor was it effective in slowing the progression of diabetes in this severely diabetic mouse model. We believe that this mouse model

presumably progressed too rapidly into a pathological phenotype which does not reflect the pathophysiology of the disease in humans. The normal progression of T2DM in humans is a slow chronic process that takes place over years. Hence, it is difficult to predict the effect that a chronic anti-amyloid antibody administration would have in humans [97].

3.7.2 Rat study I (HIP1)

Male hemizygous RIPHAT rats (CD:SD-Tg(ins2-IAPP)Soel) [66] and male Sprague Dawley wild type (WT) rats were used. A chimeric version of the antibody (NI-203.26C11-r) containing human variable domains and rat IgG2b constant regions, was generated to reduce neutralizing effects against human NI-203.26C11 in rats. Rats received weekly i.p. injections of the NI-203.26C11-r antibody (3 mg/kg) or PBS starting at 12 weeks of age for 18 weeks. Oral glucose tolerance tests (oGTT) were conducted one week before, as well as 8 and 16 weeks after the start of the treatment. Additionally, fasting blood glucose values were measured 4 and 12 weeks after chronic treatment. After 18 weeks of treatment, all rats were sacrificed, insulin and hIAPP levels were measured and histological and immunohistochemical analyses of the pancreas were performed to evaluate islet area, insulin immunoreactive pancreatic β-cell area and islet amyloid. Glucose tolerance was significantly improved after 8 and 16 weeks by NI-203.26C11-r compared to PBS treatment in RIPHAT rats. Insulin levels tended to be higher and hIAPP levels were significantly higher in RIPHAT rats treated with NI-203.26C11-r in comparison with RIPHAT rats that received PBS. There were no effects on body weight (BW), fasting blood glucose, mean islet and insulin immunoreactive area in the first conducted rat study [98].

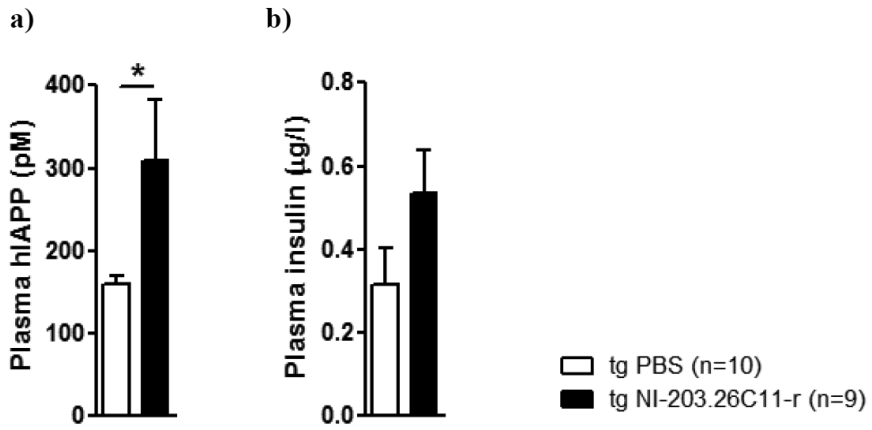

Figure 5: Rat study I (Data from M. Osto, 2014): Plasma hIAPP **(a)** and plasma insulin levels **(b)** in RIPHAT (tg) rats treated with NI-203.26C11-r antibody or PBS after 18 weeks of treatment. RIPHAT rats that received NI-203.26C11-r treatment showed significantly higher plasma hIAPP levels **(a)** and a trend for having higher plasma insulin levels **(b)**.

3.7.3 Rat study II (HIP2)

In the second rat study, RIPHAT rats (CD:SD-Tg(ins2-IAPP)Soel) [66] and wild type (WT) Sprague Dawley rats were treated for 28 weeks with the antibody NI-203.26C11-r (3 mg/kg), an isotype control IgG or PBS. Again, glucose tolerance was significantly improved after 17 weeks of treatment in RIPHAT rats that received NI-203.26C11-r compared to PBS or isotype controls. A hyperglycemic clamp performed after 20 weeks of chronic treatment showed a significant increase in insulin secretion in RIPHAT rats treated with NI-203.26C11-r compared to RIPHAT rats treated with control IgG. Fasting blood glucose was significantly reduced in NI-203.26C11-r treated RIPHAT rats compared to transgenic control rats and NI-203.26C11-r normalized fasting glucose to the levels seen in wild type rats. Control RIPHAT rats started to lose BW after 20 weeks of treatment probably due to progressive glucosuria while RIPHAT rats treated with NI-203.26C11-r continued to gain weight. The difference in BW compared to control RIPHAT rats was significant after 24 weeks of treatment. Additionally, in the histological examination of pancreatic tissue of all rats, β-cell content was significantly reduced in RIPHAT control rats compared to treated RIPHAT rats. Overall, the treatment with NI-203.26C11-r antibody improved glucose tolerance, reduced

hyperglycemia, increased plasma insulin levels, preserved β-cell content and normalized BW gain in transgenic hIAPP rats [99].

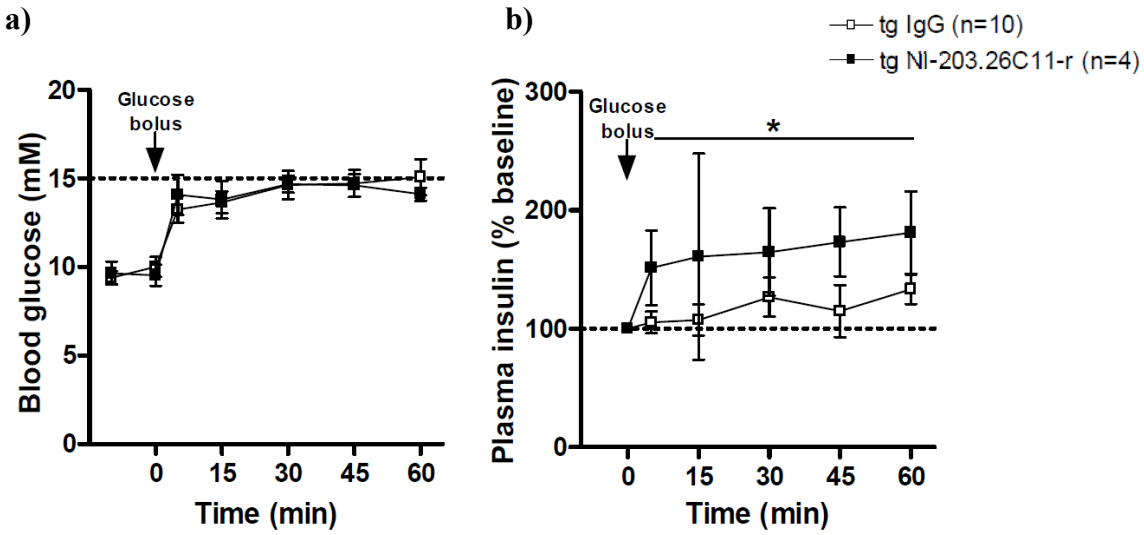

Figure 6: Rat study II (Data from M.Osto, 2015): Hyperglycemic clamp performed after 20 weeks of treatment in RIPHAT (tg) rats treated with NI-203.26C11-r antibody or IgG control. All rats received a glucose bolus (375 mg/kg) followed by 50% glucose infusion **(a)** to clamp arterial glucose at 270mg/dl (0-60 min). **(b)** Plasma insulin levels (% baseline) in RIPHAT rats treated with NI-203.26C11-r were significantly higher than in RIPHAT rats that received IgG control, indicating an increased β-cell function in NI-203.26C11-r treated rats.

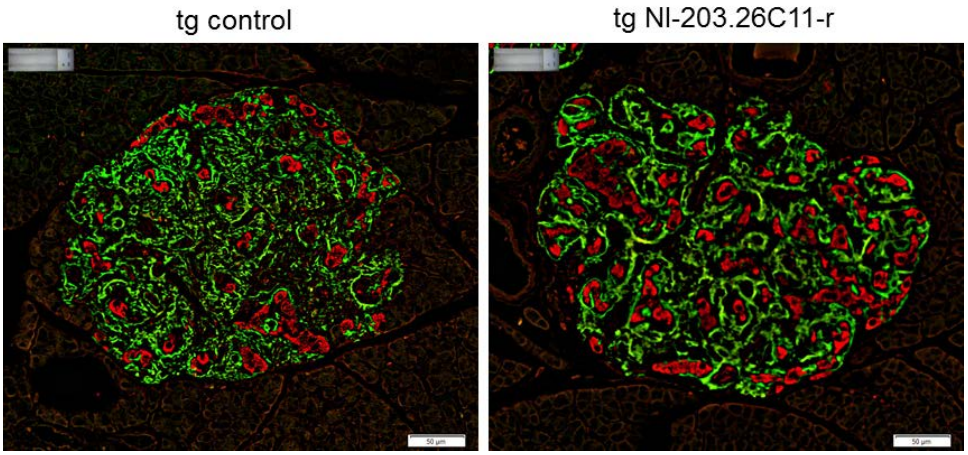

Figure 7: Representative fluorescent images of pancreatic islets in RIPHAT (tg) rats of the HIP2 study after 20 weeks of treatment. RIPHAT rat treated with vehicle control (left) showed reduced insulin staining (red) but increased ThioS-positive amyloid staining (green) compared to NI-203.26C11-r treated RIPHAT rat (right).
Scale bar: 50 µm. (Images from Neurimmune AG, Schlieren).

4 Aim of the study

The principal aim of the current study was to determine the most effective dose of NI-203.26C11-r antibody in hIAPP transgenic rats. In order to achieve this aim, three different doses (1, 3 or 10 mg/kg) of the antibody NI-203.26C11-r were administered weekly in RIPHAT rats. The efficacy of the passive immunotherapeutic approach in this dose-response study was assessed by measuring blood glucose and plasma insulin levels during oral glucose tolerance tests before and throughout the treatment period.

5 Material and Methods

5.1 Animals and housing conditions

In total, 74 hemizygous transgenic male RIPHAT rats (Crl:CD (SD)-Tg (Ins2-IAPP) 1Pfi; [66]) and 13 wild-type male Sprague-Dawley rats (WT; CR:CD (SD)) were included in the study (Charles River Laboratories, Wilmington, MA, USA). Rats were kept in a temperature controlled room (21 ± 1°C) on a 12:12 hours light/dark cycle (lights off from 2pm to 2am) with ad libitum access to standard chow (Extrudate 3436, KLIBA NAFAG, Kaiseraugst, Switzerland) and water. Rats were housed in standard cages (Type 2000P, 612x435x216mm, Tecniplast, Buguggiate, Italy), in groups of two to three animals per cage. Before starting any treatment, rats (9 weeks old) were handled every second day and given an adaptation period of 3 weeks before being randomized into treatment groups. The experiments were approved by the Veterinary Office of the Canton Zurich, Switzerland (licence nr. 143/2015).

5.2 Study design

5.2.1 Injection protocol

RIPHAT (N=74) and WT (N=13) rats were divided into four treatment groups each: Group I received phosphate buffered saline (PBS, 2 ml/kg, Gibco, Auckland, NZ), group K, G and H were administered a rat chimeric version of the human anti-hIAPP antibody: NI-203.26C11-r at 1, 3 or 10 mg/kg in 2 ml/kg PBS, respectively (see table 2 for the number of rats per group).

Intraperitoneal (i.p.) injections were initiated at 12 weeks of age and repeated weekly until the end of the experiments at 53 weeks of age. Oral glucose tolerance tests (oGTT) were performed at 12, 20, 26, 30, 34, 38, 42, 46 and 51 weeks of age. The first oGTT at 12 weeks of age was done before the start of any treatment and data collected at this time served as a baseline. Fasting glucose and insulin levels were measured during the oGTT (see paragraph 5.2.3 for details) and BW was measured weekly to monitor rats' health and to determine the injection volume.

Table 2: Total number of rats used in the study, divided into the four treatment groups I (control), K (1 mg/kg), G (3 mg/kg) and H (10 mg/kg) of NI-203.26C11-r, respectively.

Treatment	WT rats	RIPHAT rats	Total
I (PBS 2 ml/kg)	3	18	21
K (NI-203.26C11-r 1 mg/kg)	4	19	23
G (NI-203.26C11-r 3 mg/kg)	3	19	22
H (NI-203.26C11-r 10 mg/kg)	3	18	21
Total	13	74	87

5.2.2 Human anti-IAPP antibodies

Antibodies against human IAPP were produced by Neurimmune Holding AG (Schlieren, Switzerland). Reactive memory B-cells were isolated from peripheral blood of healthy human donors. Conditioned media derived from human memory B-cell cultures were screened for antibodies binding to aggregated IAPP protein and absence of binding to bovine serum albumin (BSA), using a direct ELISA approach. Only cultures of B-cells positive for aggregated IAPP protein but not for BSA were used for antibody cloning.

Selected antibodies were recombinantly produced and further analyzed for class and light chain subclass determination. These antibodies were characterized for their binding specificities towards aggregated or non-aggregated hIAPP protein by direct ELISA on 96-well plates (Costar, Corning, USA) coated with human IAPP solution which contained IAPP fibrils or BSA (Sigma-Aldrich, Buchs, Switzerland) diluted to a concentration of 10 µg/ml in carbonate ELISA coating buffer (15 mM Na_2CO_3, 35 mM $NaHCO_3$, pH 9.42). After overnight incubation at room temperature, binding efficiency of the antibodies was tested by blocking non-specific binding sites for 1 hour at room temperature with PBS/0.1% Tween-20 (polysorbate surfactant) containing 2% BSA (Sigma-Aldrich, Buchs, Switzerland).

After being transferred to ELISA plates, B-cell conditioned medium or recombinantly produced antibodies were incubated at room temperature for one hour. ELISA plates were washed in PBS-Tween 20. Binding was determined using horseradish peroxidase (HRP)-conjugated anti-human IgG polyclonal antibodies (Jackson ImmunoResearch,

Newmarket, UK). HRP activity was assessed with standard colorimetric detection using a plate reader (Sunrise ELISA reader, Tecan Group Ltd, Männedorf, Switzerland).

a) **b)**

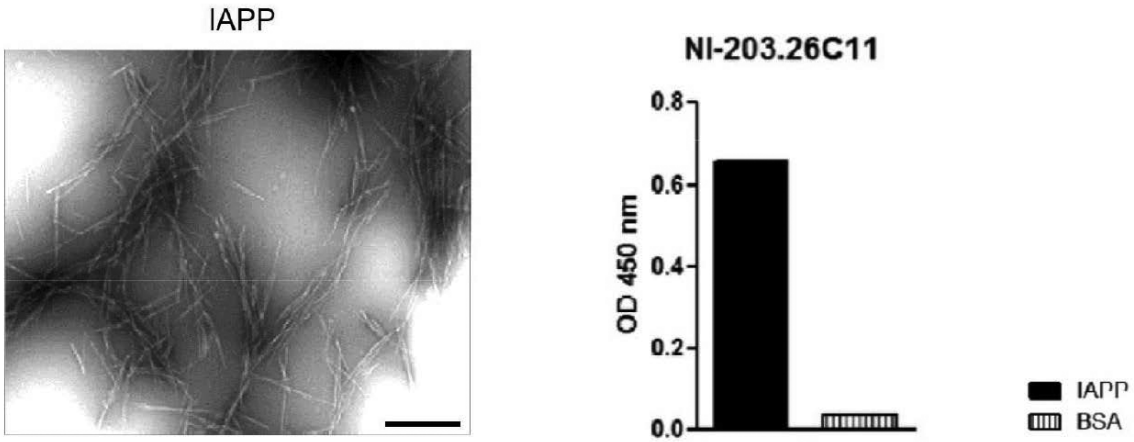

Figure 8: The binding specificity for IAPP of human recombinant antibodies assessed by direct ELISA (Data and images from Neurimmune). **(a)** Electron microscopy image of the aggregated IAPP solution (2 mg/ml) used for ELISA plate coating. Scale bar = 1 µm. **(b)** Data expressed as OD values at 450 nm showing a specific binding to human IAPP (10 µg/ml) by the recombinant antibody NI-203.26C11, but no binding to BSA (10 µg/ml).

In case B-cell conditioned medium revealed antibodies with selective binding to aggregated hIAPP, mRNA of B-cells was prepared and immunoglobulin heavy and light chains were cloned with a nested polymerase chain reaction (PCR) approach. This approach consists in a modified PCR intended to reduce non-specific binding in products due to the amplification of unexpected primer binding sites. Antibodies were identified by rescreening on ELISA upon recombinant expression of complete antibodies in Chinese Hamster Ovary (CHO) cells and using expression vectors, where variable heavy and light chain sequences "in the correct reading frame" were inserted. An Ig-heavy-chain expression vector and a kappa or lambda Ig-light-chain expression vector were used. The monoclonal antibodies were purified with standard protein A column purification and tested again for their binding properties by ELISA.

The half maximal effective concentration (EC_{50}) was examined using additional direct ELISA experiments with varying antibody concentrations. The EC_{50} values were estimated by a non-linear regression using GraphPad Prism software (San Diego, USA).

Recombinant human-derived antibody NI-203.26C11 bound with a high affinity to human IAPP aggregates with an EC50 of 6 nM.

By using another direct ELISA experiment, the binding capacity of the antibody NI-203.26C11 to conformational epitopes was defined. The antibody showed high affinity to binding to IAPP fibrils upon coating with the IAPP solution and a loss in affinity to nonfibrillar IAPP. These findings lead to the conclusion that the antibody NI-203.26C11 binds a conformational epitope predominantly exposed on aggregated IAPP species, but not to linear epitopes that are present in the physiological monomeric human IAPP protein.

To reduce a rat anti-human antibody response during the treatment, protein engineering was used to generate recombinant rat chimeric NI-203.26C11-r antibody, containing human variable domains and rat constant regions. Antibodies were purified by affinity chromatography to get endotoxin-free antibodies for *in vivo* validation.

To assess the affinity and selectivity of NI-203.26C11, fluorescent images for insulin and Thioflavin-S (amyloid deposits) of pancreatic tissue in RIPHAT rats and WT rats were performed. The presence of amyloid (Thio-S)-positive pancreatic islets was confirmed in RIPHAT but not in WT rats. Furthermore, bright field images of the same pancreatic islets of RIPHAT and WT rats were stained with NI-203.26C11 and mouse anti-IAPP antibody. NI-203.26C11 staining was observed on amyloid (Thio-S)-positive islets from RIPHAT rats binding to aggregated hIAPP, but without binding to physiological rat IAPP (rIAPP) visualized by the mouse monoclonal anti-IAPP antibody on WT rat islets. Interestingly, binding of NI-203.26C11 antibody was also seen on Thio-S-negative areas in amyloid (Thio-S)-positive islets from RIPHAT but not WT rats.

a)

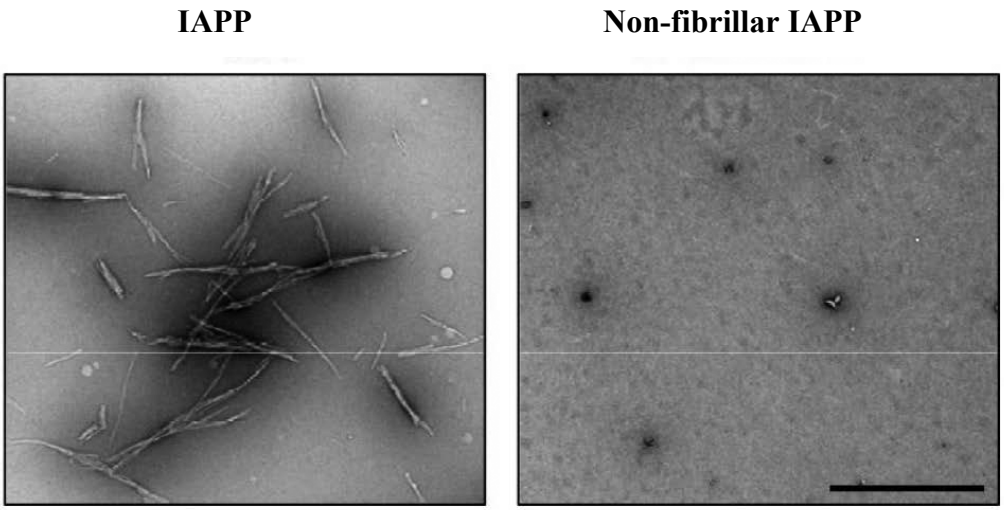

b)

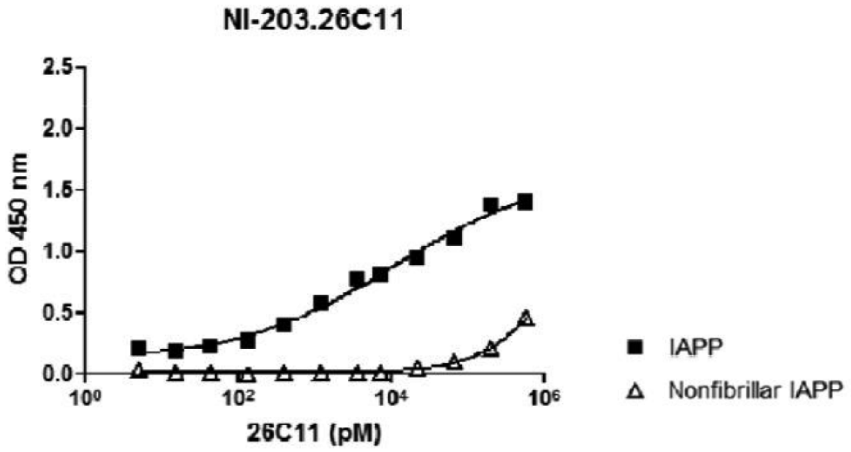

Figure 9: Anti-IAPP antibodies are specific to human IAPP fibrils (Data and images from Neurimmune). **(a)** Electron microscopy pictures of human IAPP (2mg/ml), containing fibrils, and nonfibrillar IAPP (500 µg/ml) solutions without any visible fibrils, used for ELISA plate coating. Scale bar = 1 µm. **(b)** Plates were incubated with the indicated concentrations of the recombinant human-derived antibody NI-203.26C11, and this antibody binds with high affinity to aggregated IAPP fibrils and very low affinity to nonfibrillar IAPP without any aggregates. These findings suggest specificity of the NI-203.26C11 antibody towards IAPP aggregates. Measurements were made in duplicate and background signal on BSA was subtracted. Data are expressed as mean OD values at 450 nm.

5.2.3 Oral Glucose Tolerance Test (oGTT)

OGTTs were conducted just before the beginning of the treatment at 12 weeks of age and at 8, 14, 18, 22, 26, 30, 34 and 39 weeks after the onset of treatment with NI-203.26C11-r or PBS. Fasting blood glucose was measured additionally 28, 32 and 41 weeks after the beginning of the chronic treatment.

Following a 12 hour fast (from 7pm until 7am), BW was measured and rats received a 2 g/kg glucose solution (4 ml/kg BW of 50% glucose, B. Braun, Melsungen, Germany) by oral gavage. Rats were briefly anesthetized with isoflurane (3-4%, Attane, Piramal Enterprises Limited, Mumbai, India) and blood samples (250 µl full blood/500 µl EDTA Microtainer K2E tube, Becton Dickinson, Franklin Lakes, USA) were collected by sublingual sampling before (0 min) and 15, 30, 60, 120 and 240 minutes after glucose load. Blood glucose was assessed using a Breeze2 glucometer and glucose stripes (Bayer, Diabetes Care, Zurich, Switzerland). Plasma insulin concentration was measured using a rat Insulin ELISA kit from Mercodia (Uppsala, Sweden) following the manufacturer's instructions.

5.2.4 Plasma and pancreas sampling

At 53 weeks of age, rats were anesthetized with pentobarbital (60 mg/kg, i.p.) and sacrificed by exsanguination via the vena cava caudalis. A minimum of 5 ml full blood was collected and plasma was stored at -80°C. The pancreas was collected and fixed with 4 % paraformaldehyde (PFA) solution. After 24 hours at 4°C and overnight dehydrating in Shandon Citadell 2000 (Thermo Fisher Scientific, Waltham, USA), pancreatic tissue was embedded in paraffin blocks (Leica EG1160, using paraplast from Leica Biosystems, Wetzlar, Germany), cut into 2.5 µm slides with a microtome (Leica RM2255, Leica Biosystems, Wetzlar, Germany), placed on glass slides and stored overnight at 60°C.

5.3 Statistics

All data were analyzed using GraphPad Prism 5 (San Diego, USA). One-way analysis of variances (One-way-ANOVA) with multiple comparisons was used for the analysis of fasting glucose, fasting insulin, delta-values and the area under curve (AUC) of glucose and insulin levels during the oGTTs. Bonferroni's post-test was used at One-way ANOVAs including WT and RIPHAT rats, and Dunnet's post-test at One-way

ANOVAs including only the RIPHAT rats. Two-way analysis of variances (Two-way-ANOVA) with multiple comparisons (Bonferroni's post-test) was used to analyze glucose and insulin values during the oGTTs. A *p*- value <0.05 indicated statistical significance. All data are presented as mean ± SEM.

6 Results

6.1 Animals

As described in the literature, the onset of overt diabetes in RIPHAT rats occurs between 5 and 10 months of age [66]. In our study, most RIPHAT-PBS control rats started to develop a diabetic phenotype, characterized by polyuria and polidipsia (PU/PD) and weight loss, at about 36 weeks of age. These clinical signs worsened over time but did not result in spontaneous death during the study period (up to 53 weeks of age). A similar diabetic phenotype was also observed in approximately half of the rats of the antibody-treated RIPHAT groups (RIPHAT-1 mg/kg, RIPHAT-3 mg/kg and RIPHAT-10 mg/kg) but the progression of the disease was slower and the diabetic phenotype appeared approximately one month later than in control rats (RIPHAT-PBS). One rat in the RIPHAT-3 mg/kg group had to be euthanized at the age of 48 weeks, because of its excessive weight loss that went beyond the pre-defined ethically acceptable level (> 20%).

Hence, the final number of animals was 18 RIPHAT-PBS rats, 19 RIPHAT-1 mg/kg rats, 18 RIPHAT-3 mg/kg rats, 18 RIPHAT-10 mg/kg rats and 13 WT rats receiving similar treatment options than the RIPHAT rats (3 WT-PBS rats, 4 WT-1 mg/kg rats, 3 WT-3 mg/kg rats and 3 WT-10 mg/kg rats). As expected, none of the investigated parameters differed significantly between the four different treatment options in WT rats and therefore, all four WT groups were taken together into one WT group counting 13 WT rats.

Number of oGTT	1st	2nd	3rd	4th	5th	6th	7th	8th	9th	Sacrifice
Age (weeks)	12	20	26	30	34	38	42	46	51	53
Treatment (weeks)	0	8	14	18	22	26	30	34	39	41

Figure 10: Timeline of the entire experimental period with age in weeks as well as weeks of treatment in all rats from the 1st until the 9th oGTT and at sacrifice.

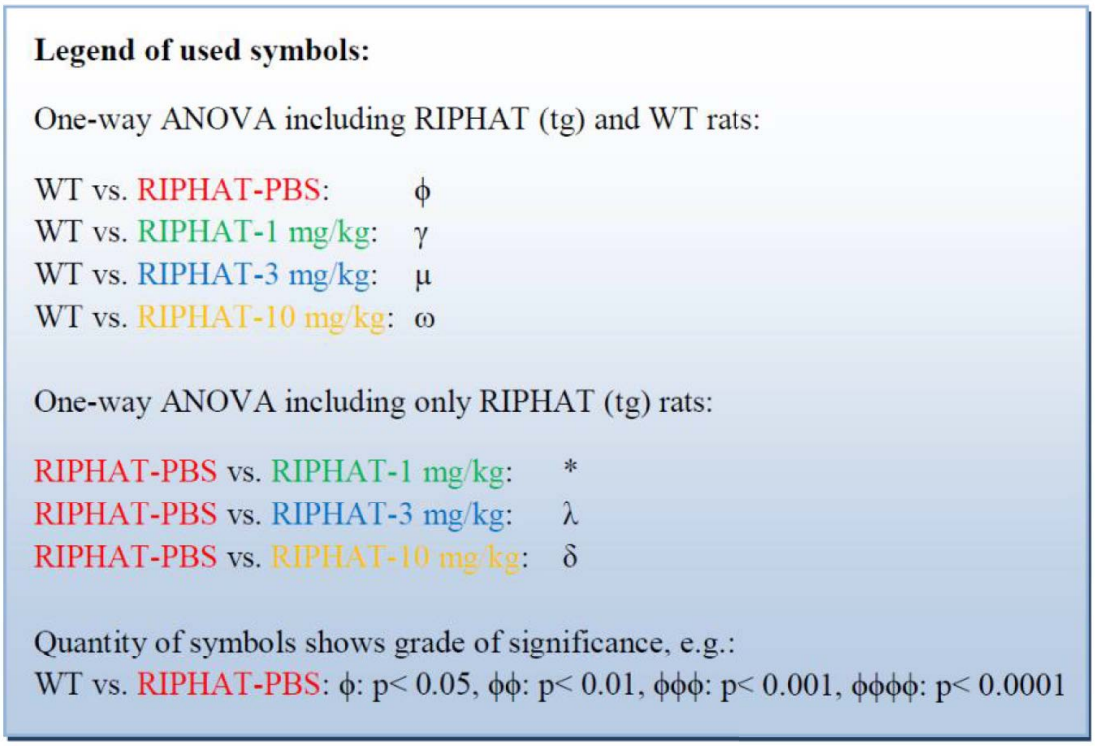

Figure 11: Legend of the symbols, used for all graphs of the study.

6.2 Body weight

Body weight (BW) was measured weekly in all rats during the entire experimental period. All rats gained weight over the first 9 months of age. WT rats continued to gain weight while antibody-treated RIPHAT rats reached a plateau in BW which they maintained until the end of the study. On the other hand, RIPHAT-PBS rats started to show a weekly decrease in BW (of around 0.5 %) from 37 weeks of age, which resulted in a total BW loss of around 8% by the end of the study at 53 weeks of age. There were no significant differences in BW between the antibody-treated groups, however, only the RIPHAT-1 mg/kg group showed a significantly increased BW compared to RIPHAT-PBS rats from 37 weeks of treatment until sacrifice (see figure 12).

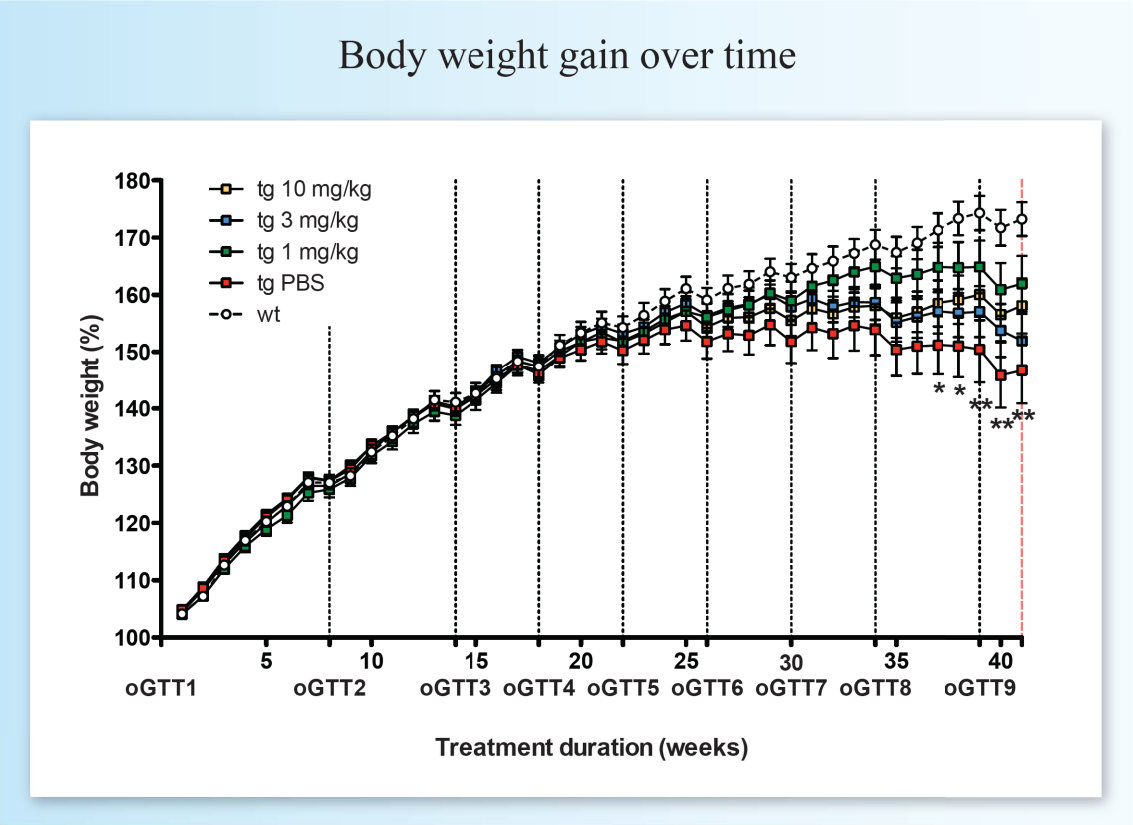

Figure 12: BW gain of WT and RIPHAT rats over time. The 2nd to the 9th oGTT are marked with black grid lines, the sacrifice is marked with a red grid line. From the beginning of the study until 24 weeks of treatment, all rats gained weight. RIPHAT(tg)-PBS rats lost weight from 25th week of treatment until sacrifice at 41 weeks of treatment, while antibody-treated RIPHAT rats (RIPHAT(tg)-1 mg/kg, RIPHAT(tg)-3 mg/kg, RIPHAT(tg)-10 mg/kg) maintained stable BW until the end of the study. See legend of the symbols for significant differences.

6.3 Fasting blood glucose and insulin levels

6.3.1 Fasting glucose levels

Fasting blood glucose (FG) levels were measured the first time in 12 week-old rats, i.e. just before the weekly antibody treatment was started. At the time of the 1st oGTT (12 weeks of age), FG was already significantly higher in RIPHAT compared to WT rats (see table 3 and figure 13a).

Significant differences in FG between WT and RIPHAT-PBS rats were seen during the entire treatment period (except at the 5th oGTT), while differences were only erratically observed between WT and RIPHAT treatment groups (see table 3).

No differences between the RIPHAT groups were observed before 22 weeks of treatment. At the 5th and the 6th oGTT, however, the treatment showed some effect

because the FG in RIPHAT-PBS rats was significantly increased compared to RIPHAT-3 mg/kg rats. Significant differences were also observed between RIPHAT-PBS and RIPHAT-1 mg/kg groups starting after 34 weeks of treatment (at the 8th oGTT) until the end of the study. The FG of RIPHAT-PBS and RIPHAT-10 mg/kg groups differed significantly only at the end of the study after 41 weeks of treatment. However, no significant differences in FG were seen between the three antibody-treatment dose groups at any time-point (see table 3 and figure 13a).

Table 3: Fasting glucose (FG) and non-fasting glucose (NFG) of WT and RIPHAT rats at different time-points of treatment. All RIPHAT rats had significantly elevated FG and NFG levels compared to WT rats during the entire study (except at 5th oGTT). However, all antibody-treated RIPHAT rats (RIPHAT-1 mg/kg, RIPHAT-3 mg/kg, RIPHAT-10 mg/kg) showed lower FG and NFG levels compared to RIPHAT-PBS control rats with significantly decreased values at several time-points. See legend of the symbols for significant differences.

Weeks of treatment	WT (mmol/L)	RIPHAT-PBS (mmol/L)	RIPHAT-1mg/kg (mmol/L)	RIPHAT-3mg/kg (mmol/L)	RIPHAT-10mg/kg (mmol/L)	Significances
0	6.8±0.2	8.0±0.2	7.8±0.2	7.9±0.2	7.7±0.3	ϕϕ, μ
8	6.5±0.2	7.8±0.3	7.3±0.3	7.5±0.3	7.3±0.3	ϕ
14	6.8±0.2	8.2±0.2	7.2±0.4	7.9±0.3	7.7±0.3	ϕ
18	7.2±0.3	8.5±0.3	7.9±0.2	8.3±0.2	8.3±0.3	ϕϕ, μ, ω
22	7.1±0.2	8.2±0.3	7.3±0.3	7.2±0.3	7.3±0.2	λ
26	6.6±0.2	8.7±0.3	8.3±0.3	7.7±0.3	8.1±0.4	ϕϕϕϕ, γγ, ωω, λ
28	6.3±0.3	8.5±0.4	7.6±0.3	8.2±0.6	8.2±0.5	ϕϕ, μ
30	6.4±0.2	9.4±0.7	7.7±0.3	8.1±0.7	8.1±0.6	ϕϕ
32	5.9±0.2	10.0±1.1	7.4±0.5	8.4±0.9	8.4±0.7	ϕϕ
34	6.6±0.3	11.4±1.0	8.0±0.6	10.2±1.0	9.8±1.0	ϕϕ, *
39	6.7±0.3	14.7±1.3	10.2±1.1	11.9±1.5	10.7±1.2	ϕϕϕ, μ, *
41	6.2±0.8	14.7±1.5	10.2±1.3	12.6±1.9	9.6±1.3	ϕϕϕ, μ, δ
41 NFG	10.4±0.4	37.8±4.1	25.7±3.5	27.8±4.3	23.8±3.2	ϕϕϕϕ, γ, μ, ω

6.3.2 Fasting insulin levels

Fasting plasma insulin levels (FI) in WT rats were higher than in RIPHAT rats at all time-points but the difference reached significance only at the 2nd oGTT and again from the 6th oGTT until sacrifice (see table 4 and figure 13b).

FI in all RIPHAT rats remained similar from the 2nd until the 8th oGTT and at sacrifice and therefore, no significant differences in FI between the four RIPHAT groups were seen at these time-points of the experimental period (see table 4). However, all three antibody treated RIPHAT groups showed a strong tendency towards higher FI levels at the 9th oGTT and non-fasting insulin levels (NFI), measured at sacrifice, in comparison with RIPHAT-PBS control rats (see table 4 and figure 13b).

Table 4: Fasting insulin (FI) and non-fasting insulin levels (NFI) of WT and RIPHAT rats at different time-points of treatment. Over the entire experimental period, WT rats showed higher FI and NFI levels compared to all RIPHAT rats. The four RIPHAT groups had constant and similar FI levels from 2nd until 8th oGTT and at sacrifice. But FI levels at 9th oGTT and NFI levels at sacrifice of RIPHAT-PBS rats tended to be lower compared to all antibody-treated RIPHAT rats (RIPHAT-1 mg/kg, RIPHAT-3 mg/kg, RIPHAT-10 mg/kg). See legend of the symbols for significant differences.

Weeks of treatment	WT (µg/L)	RIPHAT-PBS (µg/L)	RIPHAT-1mg/kg (µg/L)	RIPHAT-3mg/kg (µg/L)	RIPHAT-10mg/kg (µg/L)	Significances
8	0.28±0.03	0.18±0.01	0.16±0.01	0.18±0.01	0.22±0.02	ϕϕϕ, γγγγ, µµµ
14	0.27±0.02	0.19±0.02	0.18±0.02	0.17±0.01	0.22±0.04	
18	0.27±0.02	0.20±0.02	0.19±0.01	0.22±0.04	0.20±0.02	
22	0.33±0.03	0.29±0.03	0.25±0.01	0.27±0.01	0.30±0.01	
26	0.44±0.10	0.22±0.02	0.19±0.02	0.20±0.02	0.23±0.05	ϕ, γγ, µµ, ω
30	0.4±0.04	0.27±0.06	0.20±0.02	0.21±0.03	0.21±0.03	γγ, µµ, ωω
34	0.29±0.05	0.19±0.03	0.18±0.02	0.17±0.02	0.16±0.02	ω
39	0.44±0.08	0.13±0.02	0.21±0.03	0.21±0.05	0.21±0.04	ϕϕϕ, γγ, µµ, ωω
41	0.44±0.08	0.17±0.01	0.19±0.01	0.17±0.01	0.19±0.01	ϕϕϕϕ, γγγγ, µµµµ, ωωωω
41 NFI	7.0±0.4	1.4 ±0.5	2.7±0.5	2.7±0.7	2.7±0.6	ϕϕϕϕ, γγγγ, µµµµ, ωωωω

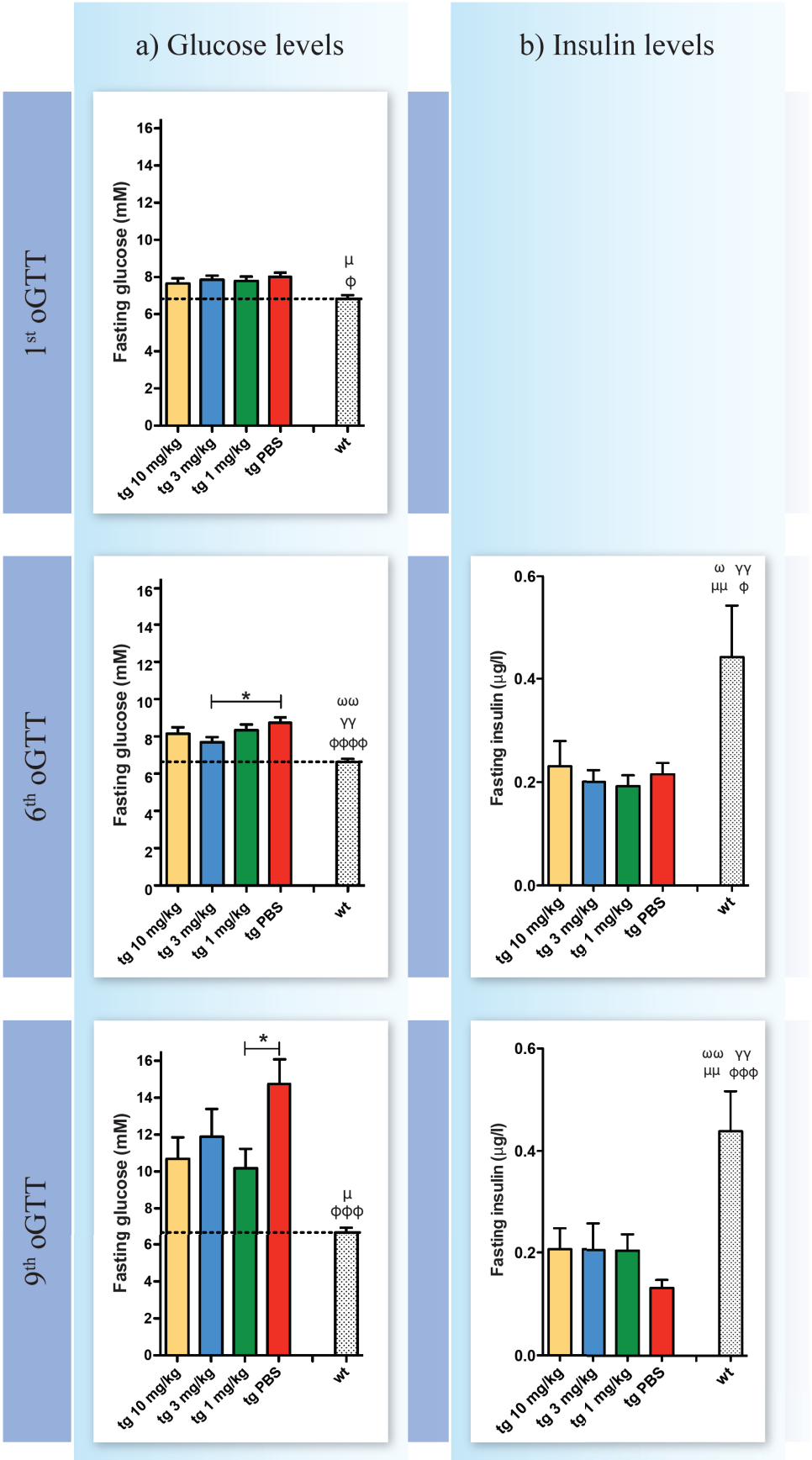
a) Glucose levels
b) Insulin levels
1st oGTT
6th oGTT
9th oGTT
Fasting glucose (mM)
Fasting insulin (µg/l)
tg 10 mg/kg
tg 3 mg/kg
tg 1 mg/kg
tg PBS
wt
µ
ϕ
*
ωω
γγ
ϕϕϕϕ
µµ
ϕϕϕ

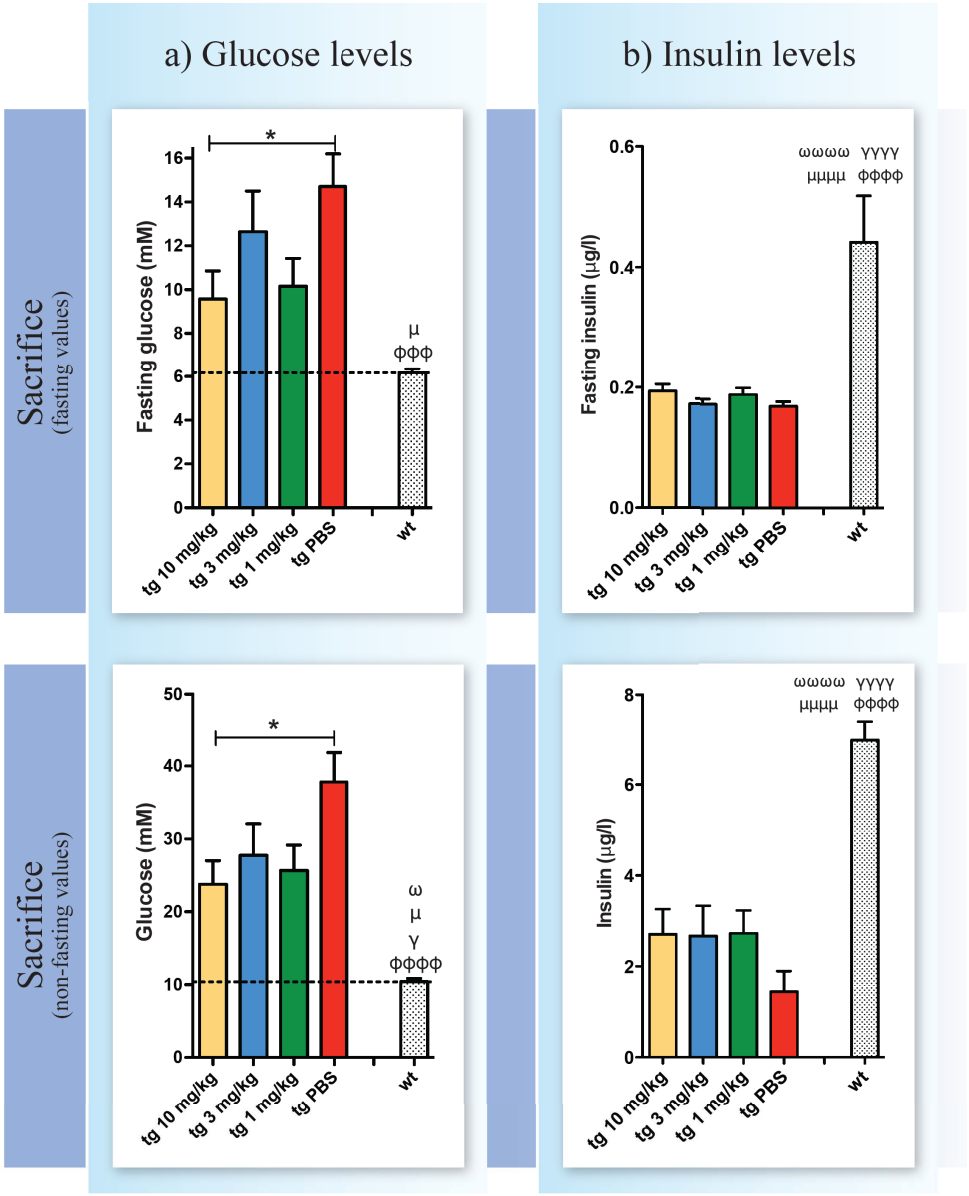

Figure 13: Fasting and non-fasting levels of glucose and insulin of RIPHAT and WT rats at 1st, 6th and 9th oGTT and at sacrifice. See legend of the symbols for significant differences.

a) Glucose levels: Dotted black line indicates the average level of glycemia in WT rats. Fasting glucose (FG) of WT rats was lower compared to RIPHAT rats during the entire experimental period and also non-fasting glucose (NFG) of WT rats at sacrifice was reduced compared to RIPHAT rats. At 1st oGTT, FG of all RIPHAT rats was similar. Until the end of the study, FG levels in all RIPHAT rats, especially in RIPHAT(tg)-PBS rats, increased over time. FG levels at 6th and 9th oGTT and at sacrifice as well as NFG levels at sacrifice of RIPHAT(tg)-PBS rats were higher compared to antibody-treated RIPHAT groups (RIPHAT(tg)-1mg/kg, RIPHAT(tg)-3 mg/kg, RIPHAT(tg)-10 mg/kg).

b) Insulin levels: Fasting insulin (FI) and non-fasting insulin (NFI) was higher in WT rats compared to RIPHAT rats at all time-points. FI levels of RIPHAT rats were similar at almost all time-points of the study, however, FI levels at 9th oGTT and NFI levels at sacrifice tended to be reduced in RIPHAT (tg)-PBS rats.

6.4 Blood levels during the oGTTs

6.4.1 Glucose levels

During the 1st oGTT before the beginning of the weekly antibody treatment, RIPHAT rats had already an impaired glucose tolerance compared to WT rats (see figure 14a). All treatment groups of RIPHAT rats showed similar baseline glycemia and glucose AUC levels during the 1st oGTT (see tables 5 and 6 and figure 14a).

During the entire experimental period, glucose intolerance progressed over time in the RIPHAT-PBS control group compared to WT rats. The progression of glucose intolerance was less severe in all RIPHAT rats which received the antibody treatment, especially in RIPHAT-1 mg/kg and RIPHAT-10 mg/kg groups (see table 5), nonetheless, their glucose curves remained elevated compared to WT rats at all time points (see figure 14a).

Differences in the glucose tolerance between the transgenic groups were seen first after 8 weeks of treatment during the 2nd oGTT, with the RIPHAT-10 mg/kg rats having lower blood glucose values at 30, 60 and 120 min compared to the control RIPHAT group (see table 5). In both RIPHAT-1 mg/kg and RIPHAT-10 mg/kg groups, glucose curves and AUC of glucose differed significantly compared to RIPHAT-PBS control rats from the 3rd until the 8th oGTT (see tables 5 and 6 and figure 14a). The progression of glucose intolerance was less influenced in the RIPHAT-3 mg/kg group compared to the RIPHAT-PBS control group, and differences in glucose values between the two groups were seen only during the 6th oGTT (see tables 5 and 6 and figure 14a).

Surprisingly, significant differences in the glucose AUC and the glucose curves were no longer observed during the last, 9th oGTT (see tables 5 and 6 and figure 14a) between any RIPHAT treatment group and their transgenic controls, though the AUC of glucose over time was significantly reduced in RIPHAT-1 mg/kg and RIPHAT-10 mg/kg rats compared to controls (see figure 15a).

Based on the AUC of glucose and the glucose curves, no significant differences were seen between the three antibody-treated RIPHAT groups during the entire experimental period (see tables 5 and 6 and figures 14a and 15a).

Table 5: Glucose levels of RIPHAT rats at different oGTTs at 0, 15, 30, 60, 120 and 240 minutes. All RIPHAT rats had similar glucose values before the start of any treatment at 1st oGTT. From the 2nd until the 9th oGTT, RIPHAT-PBS group showed the highest glucose levels, with significant differences (see legend of the symbols) compared to the antibody-treated RIPHAT groups (RIPHAT-1mg/kg, RIPHAT-3 mg/kg, RIPHAT-10 mg/kg) at different time-points of several oGTTs.

Weeks of treatment	Time-point (min)	RIPHAT-PBS (mmol/L)	RIPHAT-1mg/kg (mmol/L)	RIPHAT-3mg/kg (mmol/L)	RIPHAT-10mg/kg (mmol/L)	Significances
0 (1st oGTT)	0	8.0	7.8	8.0	7.7	
	15	12.0	11.9	11.8	11.9	
	30	13.3	13.3	13.1	13.4	
	60	12.6	13.0	12.2	12.6	
	120	10.3	10.2	10.8	10.5	
	240	9.6	8.8	9.3	9.3	
8 (2nd oGTT)	0	7.8	7.3	7.5	7.3	
	15	13.4	12.2	13.0	12.4	
	30	15.8	14.0	14.2	13.5	δ
	60	15.4	13.2	14.5	12.9	δ
	120	12.3	10.4	11.2	9.9	δ
	240	8.6	7.8	7.9	8.5	
14 (3rd oGTT)	0	8.2	7.2	7.9	7.7	
	15	14.4	12.9	13.6	13.1	
	30	16.4	14.0	14.4	14.1	*, δ
	60	17.0	14.3	15.4	13.7	**, δδδ
	120	13.8	10.7	11.8	10.8	***, δδ
	240	9.3	8.5	9.1	9.3	
18 (4th oGTT)	0	8.5	7.9	8.3	8.3	
	15	15.6	13.9	13.9	13.6	
	30	17.2	14.9	15.2	14.7	*, δ
	60	17.1	14.9	15.8	14.5	δ
	120	14.2	12.1	12.3	11.6	δ
	240	10.3	8.4	9.5	9.5	
22 (5th oGTT)	0	8.2	7.3	7.2	7.3	
	15	15.4	13.6	13.9	13.1	
	30	16.7	14.6	15.1	14.4	
	60	17.6	14.8	15.6	14.5	*, δ
	120	15.0	11.7	13.2	11.8	**, δδ
	240	10.6	8.0	9.3	9.4	*
26 (6th oGTT)	0	8.7	8.3	7.7	8.1	
	15	16.4	13.8	14.0	14.0	
	30	18.0	15.0	14.9	15.2	*, λ
	60	18.1	15.0	15.5	14.9	*, δ
	120	15.4	12.2	13.8	11.8	*, δ
	240	12.4	8.0	10.3	10.3	***
30 (7th oGTT)	0	9.4	7.7	8.1	8.1	
	15	18.1	14.5	14.8	14.5	
	30	19.1	15.7	15.6	14.8	δ
	60	19.7	15.4	16.7	14.8	*, δδ
	120	16..9	13.5	14.9.	12.8	δ
	240	14.2	9.4	11.9	11.2	**
34 (8th oGTT)	0	11.4	8.0	10.2	9.8	
	15	22.0	16.6	18.3	17.4	*
	30	24.5	19.0	21.3	19.2	*, δ
	60	23.8	17.8	21.0	19.0	**
	120	21.6	15.8	17.7	15.9	*, δ
	240	18.4	12.5	15.0	13.4	*
39 (9th oGTT)	0	14.7	10.2	11.9	10.7	
	15	23.3	18.2	19.1	18.1	
	30	24.8	20.1	20.9	19.7	
	60	24.0	19.0	20.4	19.5	
	120	22.0	17.1	18.7	17.5	
	240	18.4	14.4	15.5	13.3	

Table 6: Area under curve (AUC) of glucose at different time-points during the experimental period. All RIPHAT groups showed similar AUC before the start of any treatment at 1st oGTT (time-point 0). From the 2nd until the 9th oGTT, RIPHAT-PBS rats showed the highest AUC, with significantly reduced AUC in RIPHAT-1 mg/kg and RIPHAT-10 mg/kg groups at several time-points. See legend of the symbols for significant differences.

Weeks of treatment	RIPHAT-PBS ($mM.min^{-1}$)	RIPHAT-1mg/kg ($mM.min^{-1}$)	RIPHAT-3mg/kg ($mM.min^{-1}$)	RIPHAT-10mg/kg ($mM.min^{-1}$)	Significances
0	2610±75	2564±88	2609±70	2610±118	
8	2937±113	2551±119	2712±112	2519±106	*, δ
14	3190±147	2647±142	2892±125	2678±126	*, δ
18	3348±141	2862±126	2998±96	2867±148	*, δ
22	3443±172	2788±139	3042±133	2857±168	**, δ
26	3662±235	2855±156	3164±170	2968±192	**, δ
30	4029±276	3101±212	3443±213	3099±263	*, δ
34	5077±318	3703±276	4265±334	3856±315	**, δ
39	5182±307	4060±343	4381±371	4048±337	

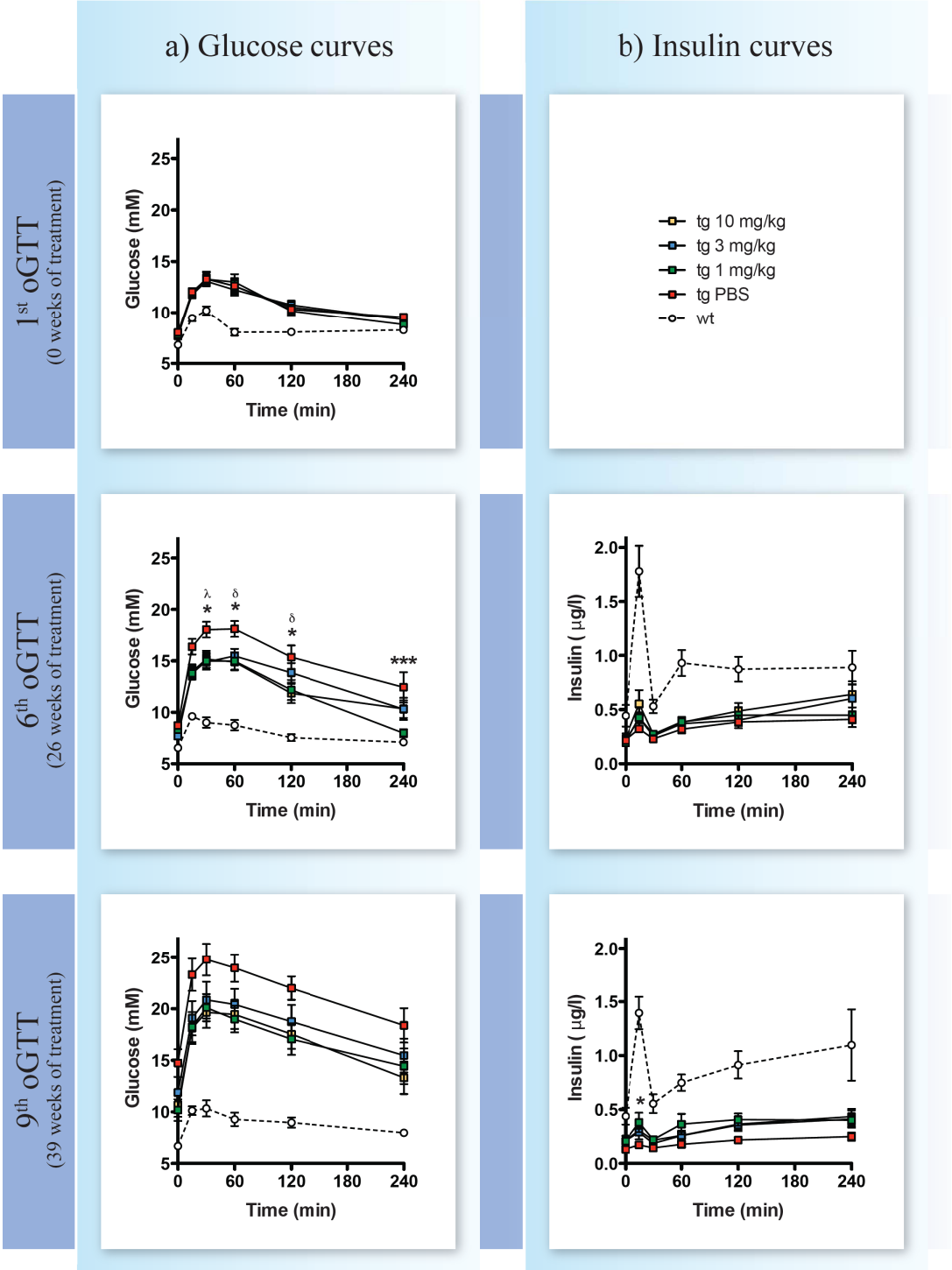

Figure 14: Glucose and insulin curves of all rats at 1st, 6th and 9th oGTT. See legend of the symbols for significant differences.

a) Glucose curves: All RIPHAT rats showed similar glucose curves at 1st oGTT before the start of any treatment. At 6th and 9th oGTT, RIPHAT-PBS control rats revealed the highest glucose values with significantly elevated glucose levels compared to the antibody-treated RIPHAT rats at different time-points of the 6th oGTT.

b) Insulin curves: Insulin levels of all RIPHAT rats were similar at 6th oGTT. At 9th oGTT, insulin levels of RIPHAT-PBS rats were lower compared to RIPHAT-1 mg/kg group.

6.4.2 Insulin levels

Reflecting the progressive decrease in β-cell function, the AUC of insulin during the oGTT decreased over time in the PBS control group. In fact, the AUC of insulin was significantly lower ($p<0.001$) at the end of the study than it was at the 2nd oGTT (see table 8 and figure 15b).

During the 2nd and 3rd oGTT, insulin values were significantly reduced in RIPHAT-PBS rats compared to RIPHAT-10 mg/kg rats while during the last three oGTTs, differences in plasma insulin levels became significant in comparison with RIPHAT-1 mg/kg rats (see table 7 and figure 14b).

However, neither the AUC of insulin nor the insulin concentrations at specific times during the oGTT were significantly different between the three antibody treated RIPHAT groups during the entire experimental period (see tables 7 and 8 and figures 14b and 15b).

Table 7: Insulin levels from the 2nd until the 9th oGTT at 0, 15, 30, 60, 120 and 240 minutes. At the 2nd and the 3rd oGTT, RIPHAT-10 mg/kg group had elevated insulin values compared to RIPHAT-PBS rats. At 7th, 8th and 9th oGTT, RIPHAT-1 mg/kg rats showed higher insulin levels compared to RIPHAT-PBS rats. See legend of the symbols for significant differences.

Weeks of treatment	Time-point (min)	RIPHAT-PBS (µg/L)	RIPHAT-1mg/kg (µg/L)	RIPHAT-3mg/kg (µg/L)	RIPHAT-10mg/kg (µg/L)	Significances
8 (2nd oGTT)	0	0.18	0.16	0.18	0.22	
	15	0.33	0.34	0.35	0.52	δδ
	30	0.17	0.19	0.17	0.28	
	60	0.33	0.31	0.32	0.40	
	120	0.38	0.37	0.40	0.56	δδ
	240	0.34	0.30	0.33	0.45	
14 (3rd oGTT)	0	0.19	0.18	0.17	0.23	
	15	0.26	0.36	0.34	0.46	δ
	30	0.23	0.30	0.27	0.32	
	60	0.41	0.48	0.43	0.53	
	120	0.51	0.52	0.46	0.64	
	240	0.45	0.45	0.49	0.66	δ
18 (4th oGTT)	0	0.21	0.19	0.23	0.20	
	15	0.31	0.35	0.31	0.35	
	30	0.20	0.25	0.21	0.22	
	60	0.29	0.35	0.32	0.32	
	120	0.39	0.39	0.45	0.43	
	240	0.39	0.42	0.46	0.48	
22 (5th oGTT)	0	0.29	0.25	0.27	0.30	
	15	0.34	0.33	0.38	0.32	
	30	0.24	0.26	0.27	0.25	
	60	0.33	0.33	0.31	0.33	
	120	0.47	0.41	0.43	0.40	
	240	0.41	0.45	0.41	0.47	
26 (6th oGTT)	0	0.22	0.19	0.20	0.23	
	15	0.32	0.43	0.42	0.55	
	30	0.23	0.27	0.26	0.27	
	60	0.32	0.39	0.37	0.38	
	120	0.39	0.45	0.40	0.49	
	240	0.41	0.45	0.60	0.64	
30 (7th oGTT)	0	0.27	0.20	0.21	0.21	
	15	0.29	0.34	0.34	0.35	
	30	0.18	0.25	0.22	0.24	
	60	0.32	0.39	0.34	0.37	
	120	0.36	0.59	0.50	0.51	*
	240	0.44	0.49	0.46	0.51	
34 (8th oGTT)	0	0.19	0.18	0.17	0.16	
	15	0.24	0.30	0.30	0.28	
	30	0.17	0.21	0.20	0.17	
	60	0.30	0.34	0.32	0.32	
	120	0.25	0.41	0.33	0.35	*
	240	0.30	0.35	0.35	0.40	
39 (9th oGTT)	0	0.13	0.21	0.27	0.21	
	15	0.17	0.38	0.29	0.31	*
	30	0.14	0.22	0.19	0.22	
	60	0.18	0.36	0.26	0.26	
	120	0.22	0.41	0.36	0.37	
	240	0.25	0.40	0.41	0.43	

Table 8: Area under curve (AUC) of insulin in RIPHAT rats at different time-points of the experimental period. While antibody-treated RIPHAT rats (RIPHAT-1 mg/kg, RIPHAT-3 mg/kg and RIPHAT-10 mg/kg) maintained stable AUCs from 2nd until 9th oGTT, the AUC of RIPHAT-PBS rats decreased over time, with lowest AUC at the end of the study (t-test of insulin AUC at 2nd oGTT and insulin AUC at 9th oGTT: $p<0.001$). See legend of the symbols for significant differences.

Weeks of treatment	RIPHAT-PBS (µg/L.min^{-1})	RIPHAT-1mg/kg (µg/L.min^{-1})	RIPHAT-3mg/kg (µg/L.min^{-1})	RIPHAT-10mg/kg (µg/L.min^{-1})	Significances
8	79.3±5.0	75.2±5.1	81.0±8.8	111.4±12.6	δ
14	102.2±8.4	108.9±9.6	102.1±9.2	136.8±13.3	
18	82.1±6.3	87.8±7.6	93.7±13.7	94.2±10.5	
22	94.9±8.8	91.5±6.9	90.4±9.8	92.2±7.8	
26	84.8±9.4	98.8±12.5	102.8±14.0	115.6±16.5	
30	83.4±10.1	112.1±14.4	99.3±14.7	105.4±10.9	
34	62.9±9.5	84.1±8.7	75.8±10.7	79.0±10.9	
39	49.4±5.9	89.3±13.1	78.5±12.7	81.7±11.6	*

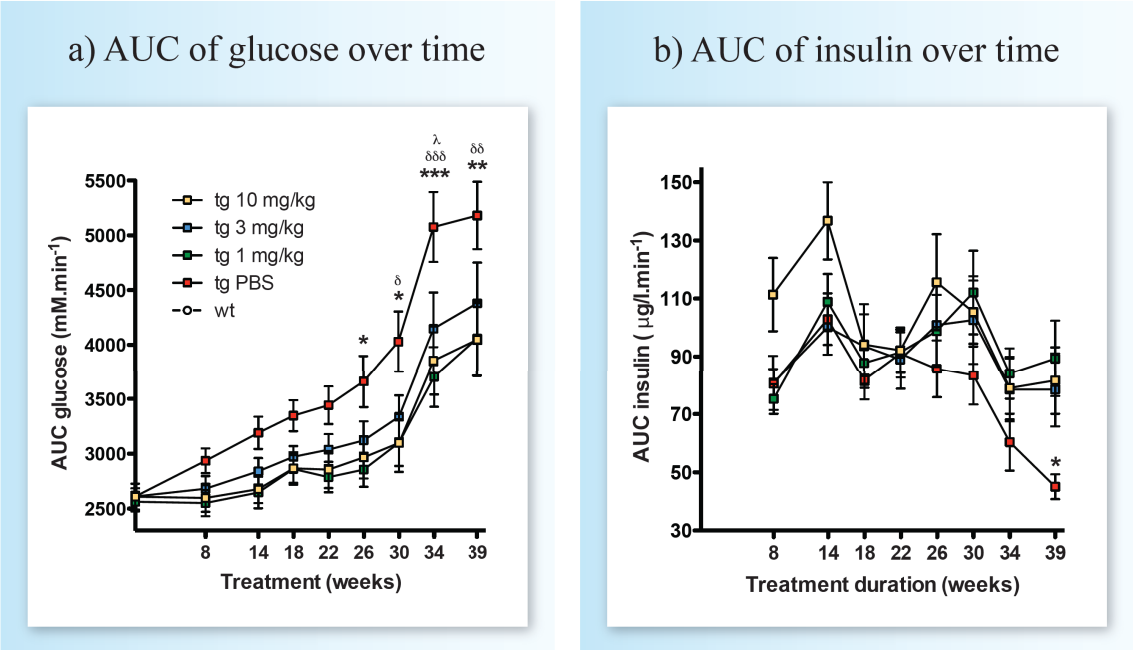

Figure 15: AUC of glucose and insulin over time in RIPHAT rats. While AUC of glucose in RIPHAT(tg)-PBS rats increased at its most, AUC of insulin in RIPHAT(tg)-PBS rats decreased over time. See legend of the symbols for significant differences.

a) Glucose AUC from 1st until 9th oGTT: AUC of glucose increased in all four RIPHAT groups over time. RIPHAT(tg)-PBS rats showed the highest AUC during all oGTTs, with significant differences compared to all antibody-treated RIPHAT rats (RIPHAT(tg)-1 mg/kg, RIPHAT(tg)-3 mg/kg, RIPHAT(tg)-10 mg/kg) at several time-points, especially at the end of the study.

b) Insulin AUC from 2nd until 9th oGTT: AUC of insulin in RIPHAT rats which received antibody treatment (RIPHAT-1 mg/kg, RIPHAT-3 mg/kg, RIPHAT-10 mg/kg) remained stable while AUC of RIPHAT(tg)-PBS rats significantly decreased until the end of the study (t-test of insulin AUC at 2nd oGTT and insulin AUC at 9th oGTT: $p<0.001$).

7 Discussion

The aim of our study was to determine the most effective dose (1, 3 or 10 mg/kg) of a human-derived antibody targeting toxic hIAPP oligomers in RIPHAT rats, a transgenic rat model of T2DM expressing hIAPP [66]. After 41 weeks of treatment with the antibody NI-203.26C11-r, all doses showed a significant effect in slowing the progression of T2DM in RIPHAT rats compared to PBS-treated RIPHAT controls based on glucose and insulin levels during the oGTTs, although no dose-dependent effects of NI-203.26C11-r were observed at the end of the experimental period.

Human T2DM is characterized by insulin resistance, defective insulin secretion due to failure and loss of pancreatic β-cells and by the deposition of islet amyloid derived from IAPP. Compensatory mechanisms of insulin resistance initially cause an increase in β-cell mass with enhanced insulin secretion [6]. Because IAPP is stored and co-secreted with insulin by the β-cells, an increase in insulin secretion also leads to an increase in IAPP secretion. Elevated IAPP concentrations in the secretory vesicles of β-cells favour the intracellular formation of small toxic IAPP oligomers, finally resulting in extracellular amyloid deposits as seen in over 90% of T2DM patients [6], [37], [41]. Toxic oligomers of IAPP cause β-cell failure and death via different mechanisms such as inflammation and membrane disruption [38], [47]. Therefore, treatment against toxic IAPP oligomers and islet amyloid deposits in diabetic patients is a very promising approach for the therapy of T2DM.

In contrast to humans, the formation of toxic IAPP oligomers does not occur in rodents because of the presence of three proline residues which act as β-sheet breakers in the amyloidogenic region of IAPP, i.e. between amino acids 20 and 29 of the 37 amino acid peptide (IAPP20-29) [35], [46]. Due to these small but important differences in the primary structure of IAPP among species, a transgenic rat model producing hIAPP in β-cells (RIPHAT rats) has been created to study the pathological mechanisms of T2DM, including the deposition of small toxic oligomers and islet amyloid in rodents [59], [66].

RIPHAT rats were used in the current study (HIP3) and in two previous studies (HIP1 and HIP2) to test the therapeutic efficacy and to establish the dose-dependent effect of

the NI-203.26C11-r antibody. This antibody has been demonstrated to bind only to pathologically misfolded but not to physiological monomeric forms of human and rat IAPP (Data from Neurimmune). RIPHAT rats represent a model of T2DM with impaired glucose tolerance around 3 months of age and a diabetic phenotype between 5 to 10 months of age; the diabetic phenotype is mainly due to the defect in insulin secretion, not insulin resistance.

In the previous studies (HIP1 and HIP2) conducted by our group in collaboration with Neurimmune AG, the 28 week administration of 3 mg/kg of the NI-203.26C11-r antibody was safe and resulted in improved glucose tolerance, enhanced β-cell function, decreased hyperglycemia, elevated plasma insulin levels, preserved β-cell content and normalized BW gain in RIPHAT rats [98], [99]. These findings were generally confirmed in the current dose-response study (HIP3), where we compared the effects of the 3 mg/kg dose to a lower (1 mg/kg) and a higher (10 mg/kg) dose of NI-203.26C11-r. RIPHAT rats treated with PBS served as control. To exclude any unspecific effect of our antibody in healthy, non-transgenic rats, WT rats received similar treatment options as the RIPHAT rats.

In the current HIP3 study, the even longer administration (41 weeks) of a higher dose (10 mg/kg) of the NI-203.26C11-r antibody was safe and had no side effects in both RIPHAT and WT rats. The observed beneficial effects basically recapitulated our previous findings because NI-203.26C11-r increased the well-being of treated RIPHAT rats, i.e. BW increased and reached a plateau during the last four months of the experimental period at all doses tested while RIPHAT-PBS control rats lost weight during the last months of the study. The latter was most likely due to the development of a severe diabetic phenotype characterized by polyuria and polydipisa (PU/PD). Interestingly, only RIPHAT rats receiving the lower antibody-dose showed a significantly higher BW gain compared to RIPHAT-PBS rats. Hence, although no significant differences were seen among the three different antibody dose groups, the RIPHAT-1 mg/kg rats tended to gain more weight compared to the other two treatment groups at the end of the study.

Fasting glucose (FG) levels in WT rats did not change and were lower compared to the RIPHAT groups during the entire experimental period. As expected, RIPHAT-PBS rats showed highest FG values among all transgenic rats, and the difference became

significant after 22 weeks (RIPHAT-3 mg/kg group), 34 weeks (RIPHAT-1 mg/kg group) or 41 weeks (RIPHAT-10 mg/kg group) of treatment, respectively. At sacrifice, the RIPHAT-10 mg/kg rats also showed significantly lower non-fasting glucose (NFG) levels compared to the control group. Therefore, consistent with the findings in the HIP2 study [99], these results showed a clear effect of the antibody in reducing FG as well as the NFG in RIPHAT rats.

Glucose intolerance in RIPHAT rats is caused by decreased β-cell mass due to toxic hIAPP oligomers which ultimately results in reduced insulin-secretion [6], [7], [66]. Thus, it is not surprising that WT rats containing a normal amount of β-cells had higher fasting insulin (FI) levels at all time-points as well as higher non-fasting insulin (NFI) levels than RIPHAT rats. Since the major function of insulin is to lower the blood glucose levels after it raises [11], NFI might serve as a better indicator of glucose intolerance than FI levels. In antibody-treated RIPHAT rats, FI levels at the 9th oGTT (i.e. after 39 weeks of treatment) and NFI levels at sacrifice were almost twice as high than in PBS-treated control rats, although differences were not significant. The higher FI and NFI levels in the antibody-treated RIPHAT rats compared to the PBS-treated control group might result from the protective effects of NI-203.26C11-r on pancreatic β-cells in reducing the aggregation of toxic hIAPP. This explanation is supported by the histological findings of the HIP2 study [99], where the β-cell content in antibody-treated RIPHAT rats was significantly larger than in PBS-treated RIPHAT control rats.

As expected in this rat model, all RIPHAT rats already showed a mild glucose intolerance during the first oGTT before the start of any treatment, i.e. at 12 weeks of age. While RIPHAT-PBS rats showed a strong progression of glucose intolerance during the experiments, the impairment of glucose tolerance was less severe in the antibody-treated RIPHAT rats. Although differences in glucose levels during the nine oGTTs were not consistently observed, overall the AUCs of glucose were lower in RIPHAT-1 mg/kg and RIPHAT 10/mg/kg groups compared to the control rats from the 2nd until the 8th oGTT. Differences between the RIPHAT-3 mg/kg rats and the PBS-control rats during the oGTTs became significant only after 34 weeks of treatment. To assess differences between the three antibody-treated dose groups, delta-values of each single dose group and the PBS-control group of the glucose and insulin results of the

study were compared by using a one-way ANOVA. Delta-values showed no significant differences in glucose levels and glucose AUCs among the three dose groups.

During the oGTTs of the first three months of the study, the RIPHAT-10 mg/kg group clearly showed higher insulin values compared to the other RIPHAT groups although differences were significant only when compared to RIPHAT-PBS rats. After 3 months of treatment, insulin levels in the RIPHAT-10 mg/kg group dropped to the levels observed in the RIPHAT-1 mg/kg and RIPHAT-3 mg/kg groups and were maintained stable until the end of the study. This trend might be explained by the fact that the highest dose of the NI-203.26C11-r antibody had the strongest protective effect against toxic hIAPP species during the initial stage of hIAPP aggregation but that with increasing amounts of aggregated hIAPP, the effect was no longer stronger than in the other antibody-treated RIPHAT groups. All antibody-treated RIPHAT groups showed higher insulin levels compared to RIPHAT-PBS rats whose insulin levels progressively decreased during the last four months of the study. This finding suggests a protective effect of the NI-203.26C11-r antibody on β-cells and insulin secretion. Despite higher insulin levels in the RIPHAT-10 mg/kg group at the beginning of the study, the comparison of the delta-values of the insulin results during the study showed no differences among the three dose groups.

To reduce an anti-antibody response against the human-derived antibody NI-203.26C11 in rats, a rat chimeric version (-r) with human variable domains and rat constant regions was produced at Neurimmune and used in this study. Nonetheless, an anti- NI-203.26C11-r antibody response that was proportional to the dose of NI-203.26C11-r injected was detected in RIPHAT rats (Data from Neurimmune; results not shown). These anti-NI-203.26C11-r antibodies might be the reason for the lack of a clear dose-dependent response in the HIP3 study because the anti-antibodies may have partly inhibited the effect of the NI-203.26C11-r antibody.

A limitation of the RIPHAT rat model is the fact that the rats do not develop insulin resistance which is an important component of most cases of T2DM in obese patients [12]. Hence, even though RIPHAT rats are a very useful model to study hIAPP aggregates in diabetes research, these rats do not fully mimic all aspects of the disease in humans.

Another potential drawback of pre-clinical studies performed in laboratory rodents is the variability and the potential appearance of (side-) effects of a compound when this is then tested in a different species. As for an example, the humanized antibody Bapineuzumab, which, despite its promising effect shown in mice in targeting the amyloid deposits derived from amyloid-β (Aβ) [100], lead to vasogenic edemas when tested in humans [101], [102], [103], [104]. Bapineuzumab was, however, a murine antibody that was humanized for the application in human patients. On the contrary, the antibody NI-203.26C11 is an antibody recombinantly produced from a human-derived antibody. We, therefore, do not expect similar drawbacks when NI-203.26C11 will be tested in humans in future clinical trials.

In summary, we demonstrated that all three tested doses of NI-203.26C11-r reduced hyperglycemia, improved glucose tolerance and increased plasma insulin levels and the low dose (1 mg/kg) even normalized BW gain. More significant differences in the AUC of glucose and in the insulin levels measured during the oGTTs were shown between the 1 mg/kg and the 10 mg/kg doses than in the 3 mg/kg dose compared to the controls. Thus, there seems to be a tendency for the low and the high antibody dose to be more effective in slowing the progression of T2DM in RIPHAT rats than the middle dose of 3 mg/kg.

Our finding that a low dose of 1 mg/kg of the antibody NI-203.26C11-r was at least as effective in slowing the progression of T2DM as a higher dose, also indicates that this dose may be sufficient for future clinical tests, reducing the potential risk for side effects as well as the higher costs when using higher doses. Further, it would be important to investigate whether even lower doses than 1 mg/kg may be sufficient to successfully slow the progression of T2DM in transgenic RIPHAT rats.

Currently, the histological examination of the pancreatic tissues of all RIPHAT and WT rats of the HIP3 study is ongoing. These additional results will add further evidences in respect to the mechanisms of action of NI-203.26C11-r in RIPHAT rats. A follow-up study has been initiated to evaluate the efficacy of a combination therapy of NI-203.26C11-r together with metformin, which is a first-line-therapy to lower blood glucose levels in diabetic human patients [67].

To conclude, passive immunization targeting IAPP aggregates with the antibody NI-203.26C11 is a very promising approach to treat T2DM.

8 References

[1] G. Danaei *et al.*, "National, regional, and global trends in fasting plasma glucose and diabetes prevalence since 1980: Systematic analysis of health examination surveys and epidemiological studies with 370 country-years and 2.7 million participants," *Lancet*, vol. 378, no. 9785, pp. 31–40, 2011.

[2] J. E. Shaw, R. A. Sicree, and P. Z. Zimmet, "Global estimates of the prevalence of diabetes for 2010 and 2030," *Diabetes Res. Clin. Pract.*, vol. 87, no. 1, pp. 4–14, 2010.

[3] L. Chen, D. J. Magliano, and P. Z. Zimmet, "The worldwide epidemiology of type 2 diabetes mellitus-present and future perspectives.," *Nat. Rev. Endocrinol.*, vol. 8, no. 4, pp. 228–36, 2012.

[4] N. H. Cho *et al.*, *IDF Diabetes Atlas*, Seventh Ed. 2015.

[5] N. Eckel, K. Mühlenbruch, K. Meidtner, H. Boeing, N. Stefan, and M. B. Schulze, "Characterization of metabolically unhealthy normal-weight individuals: Risk factors and their associations with type 2 diabetes," *Metabolism.*, vol. 64, no. 8, pp. 862–871, 2015.

[6] L. Haataja, T. Gurlo, C. J. Huang, and P. C. Butler, "Islet amyloid in type 2 diabetes, and the toxic oligomer hypothesis," *Endocr. Rev.*, vol. 29, no. 3, pp. 303–316, 2008.

[7] C. A. Jurgens *et al.*, "B-Cell Loss and B-Cell Apoptosis in Human Type 2 Diabetes Are Related To Islet Amyloid Deposition.," *Am. J. Pathol.*, vol. 178, no. 6, pp. 2632–40, 2011.

[8] M. Y. Donath and S. E. Shoelson, "Type 2 diabetes as an inflammatory disease," *Nat Rev Immunol*, vol. 11, no. 2, pp. 98–107, 2011.

[9] K. Kupsal, S. Mudigonda, and K. K. Gundapaneni, "Glucotoxicity and lipotoxicity induced beta-cell apoptosis in type 2 diabetes mellitus," *Int. J. Anal. Bio-Science*, vol. 3, no. 4, pp. 84–89, 2015.

[10] A. Mukherjee, D. Morales-Scheihing, P. C. Butler, and C. Soto, "Type 2 diabetes as a protein misfolding disease," *Trends Mol. Med.*, vol. 21, no. 7, pp. 439–449, 2015.

[11] S. Seino, "Cell signalling in insulin secretion: the molecular targets of ATP , cAMP and sulfonylurea," *Diabetologia*, vol. 55, pp. 2096–2108, 2012.

[12] M. Stumvoll, B. J. Goldstein, and T. W. Van Haeften, "Type 2 diabetes: principles of pathogenesis and therapy," *Lancet*, vol. 365, pp. 1333–1346, 2010.

[13] P. Rorsman and M. Braun, "Regulation of Insulin Secretion in Human Pancreatic Islets," *Annu. Rev. Physiol.*, vol. 75, pp. 155–179, 2013.

[14] M. Komatsu, M. Takei, H. Ishii, and Y. Sato, "Glucose-stimulated insulin secretion: A newer perspective," *J. Diabetes Investig.*, vol. 4, no. 6, pp. 511–516, 2013.

[15] A. Wiederkehr and C. B. Wollheim, "Molecular and Cellular Endocrinology Mitochondrial signals drive insulin secretion in the pancreatic b -cell," *Mol. Cell. Endocrinol.*, vol. 353, no. 1–2, pp. 128–137, 2012.

[16] J. E. Pessin and A. R. Saltiel, "Signaling pathways in insulin action: molecular targets of insulin resistance," *J. Clin. Invest.*, vol. 106, no. 2, pp. 165–169, 2000.

[17] S. E. Kahn, M. E. Cooper, and S. Del Prato, "Pathophysiology and treatment of type 2 diabetes: Perspectives on the past, present, and future," *Lancet*, vol. 383, no. 9922, pp. 1068–1083, 2014.

[18] R. P. Robertson, J. Harmon, P. O. T. Tran, and V. Poitout, “Oxidative Stress in Type 2 Diabetes,” *Diabetes*, vol. 53, no. February 2004, pp. 119–124, 2014.
[19] T. D. O’Brien, P. C. Butler, P. Westermark, and K. H. Johnson, “Islet amyloid polypeptide: a review of its biology and potential roles in the pathogenesis of diabetes mellitus,” *Vet Pathol*, vol. 30, no. 4, pp. 317–332, 1993.
[20] A. A. Young, “Amylin’s physiology and its role in diabetes,” *Curr. Opin. Endocrinol. Diabetes*, vol. 4, no. 4, pp. 282–290, 1997.
[21] P. Westermark, A. Andersson, and G. T. Westermark, “Islet amyloid polypeptide, islet amyloid, and diabetes mellitus.,” *Physiol. Rev.*, vol. 91, no. 3, pp. 795–826, 2011.
[22] L. Caillon, A. R. F. Hoffmann, A. Botz, and L. Khemtemourian, “Molecular structure, membrane interactions, and toxicity of the islet amyloid polypeptide in type 2 diabetes mellitus,” *J. Diabetes Res.*, vol. 2016, pp. 1–13, 2015.
[23] P. Westermark, C. Wernstedt, E. Wilander, and K. Sletten, “A novel peptide in the calcitonin gene related peptide family as an amyloid fibril protein in the endocrine pancreas,” *Biochem. Biophys. Res. Commun.*, vol. 140, no. 3, pp. 827–831, 1986.
[24] D. L. Hay, S. Chen, T. A. Lutz, D. G. Parkes, and J. D. Roth, “Amylin: Pharmacology , Physiology , and Clinical Potential,” *Pharmacol. Rev.*, vol. 67, no. July, pp. 564–600, 2015.
[25] A. A. Young, “Inhibition of gastric emptying,” *Adv. Pharmacol.*, vol. 52, pp. 99–121, 2005.
[26] T. a Lutz, “The role of amylin in the control of energy homeostasis.,” *Am. J. Physiol. Regul. Integr. Comp. Physiol.*, vol. 298, no. 6, pp. R1475-84, 2010.
[27] T. A. Lutz, “Control of energy homeostasis by amylin,” *Cell. Mol. Life Sci.*, vol. 69, no. 12, pp. 1947–1965, 2012.
[28] P. Y. Wielinga, C. Löwenstein, S. Muff, M. Munz, S. C. Woods, and T. A. Lutz, “Central amylin acts as an adiposity signal to control body weight and energy expenditure,” *Physiol. Behav.*, vol. 101, no. 1, pp. 45–52, 2010.
[29] D. R. Poyner *et al.*, “International Union of Pharmacology. XXXII. The mammalian calcitonin gene-related peptides, adrenomedullin, amylin, and calcitonin receptors.,” *Pharmacol. Rev.*, vol. 54, no. 2, pp. 233–246, 2002.
[30] D. L. Hay, G. Christopoulos, A. Christopoulos, D. R. Poyner, and P. M. Sexton, “Pharmacological discrimination of calcitonin receptor: receptor activity-modifying protein complexes,” *Mol Pharmacol*, vol. 67, no. 5, pp. 1655–1665, 2005.
[31] C. Betsholtz *et al.*, “Islet amyloid polypeptide (IAPP):cDNA cloning and identification of an amyloidogenic region associated with the species-specific occurrence of age-related diabetes mellitus.,” *Exp. Cell Res.*, vol. 183, no. 2, pp. 484–493, 1989.
[32] C. Betsholtz *et al.*, “Sequence divergence in a specific region of islet amyloid polypeptide (IAPP) explains differences in islet amyloid formation between species,” *FEBS Lett.*, vol. 251, no. 1–2, pp. 261–264, 1989.
[33] P. Westermark, C. Wernstedt, T. D. O’Brien, D. W. Hayden, and K. H. Johnson, “Islet amyloid in type 2 human diabetes mellitus and adult diabetic cats contains a novel putative polypeptide hormone.,” *Am. J. Pathol.*, vol. 127, no. 3, pp. 414–417, 1987.
[34] K. H. Johnson, T. D. O’Brien, C. Betsholtz, and P. Westermark, “Islet amyloid, islet amyloid polypeptide, and diabetes mellitus,” *N. Engl. J. Med.*, vol. 321, no. 8, pp. 513–518, 1989.

[35] D. F. Moriarty and D. P. Raleigh, “Effects of sequential proline substitutions on amyloid formation by human amylin20-29,” *Biochemistry*, vol. 38, no. 6, pp. 1811–1818, 1999.
[36] C. Betsholtz *et al.*, “Structure of cat islet amyloid polypeptide and identification of amino acid residues of potential significance for islet amyloid formation,” *Diabetes*, vol. 39, no. January, pp. 118–122, 1990.
[37] A. Clark and M. R. Nilsson, “Islet amyloid: A complication of islet dysfunction or an aetiological factor in Type 2 diabetes?,” *Diabetologia*, vol. 47, no. 2, pp. 157–169, 2004.
[38] A. Abedini and A. M. Schmidt, “Mechanisms of islet amyloidosis toxicity in type 2 diabetes,” *FEBS Lett.*, vol. 587, no. 8, pp. 1119–1127, 2013.
[39] E. L. Opie, “The relation of diabetes mellitus to lesions of the pancreas. Hyaline degeneration of the islands of langerhans.,” *J. Exp. Med.*, vol. 5, pp. 527–541, 1901.
[40] J. Janson, R. H. Ashley, D. Harrison, S. McIntyre, and P. C. Butler, “The mechanism of islet amyloid polypeptide toxicity is membrane disruption by intermediate-sized toxic amyloid particles,” *Diabetes*, vol. 48, no. 3, pp. 491–498, 1999.
[41] C. Lin *et al.*, “Toxic Human Islet Amyloid Polypeptide (h-IAPP) Oligomers Are Intracellular , and Vaccination to Induce Anti-Toxic Oligomer Antibodies Does Not Prevent h-IAPP-Induced B-Cell Apoptosis in h-IAPP Transgenic Mice,” *Diabetes*, vol. 56, no. May, pp. 1324–1332, 2007.
[42] P. Cao *et al.*, “Islet amyloid: From fundamental biophysics to mechanisms of cytotoxicity,” *FEBS Lett.*, vol. 587, no. 8, pp. 1106–1118, 2013.
[43] A. V Matveyenko, T. Gurlo, M. Daval, A. E. Butler, and P. C. Butler, “Successful Versus Failed Adaptation to High-Fat Diet – Induced Insulin Resistance,” *Diabetes*, vol. 58, no. April, pp. 906–916, 2009.
[44] R. L. Hull, G. T. Westermark, P. Westermark, and S. E. Kahn, “Islet amyloid: A critical entity in the pathogenesis of type 2 diabetes,” *J. Clin. Endocrinol. Metab.*, vol. 89, no. 8, pp. 3629–3643, 2004.
[45] D. T. Meier *et al.*, “The S20G substitution in hIAPP is more amyloidogenic and cytotoxic than wild-type hIAPP in mouse islets,” *Diabetologia*, vol. 59, no. 10, pp. 2166–2171, 2016.
[46] E. T. A. S. Jaikaran and A. Clark, “Islet amyloid and type 2 diabetes: From molecular misfolding to islet pathophysiology,” *Biochim. Biophys. Acta - Mol. Basis Dis.*, vol. 1537, no. 3, pp. 179–203, 2001.
[47] T. Gurlo *et al.*, “Evidence for Proteotoxicity in β Cells in Type 2 Diabetes,” *Am. J. Pathol.*, vol. 176, no. 2, pp. 861–869, 2010.
[48] G. Bhak, Y. J. Choe, and S. R. Paik, “Mechanism of amyloidogenesis: Nucleation-dependent fibrillation versus double-concerted fibrillation,” *BMB Rep.*, vol. 42, no. 9, pp. 541–551, 2009.
[49] C. Huang, C. Lin, L. Haataja, and T. Gurlo, “High expression rates of human islet amyloid polypeptide induce endoplasmic reticulum stress–mediated β-cell apoptosis, a characteristic of humans with type 2 but not type 1 diabetes,” *Diabetes*, vol. 56, no. August 2007, pp. 2016–2027, 2007.
[50] A. H. Wyllie, “‘where, o death, is thy sting?’ A brief review of apoptosis biology,” *Mol. Neurobiol.*, vol. 42, no. 1, pp. 4–9, 2010.
[51] J. da Rocha Fernandes *et al.*, “IDF Diabetes Atlas estimates of 2014 global health expenditures on diabetes,” *Diabetes Res. Clin. Pract.*, vol. 117, pp. 48–54, 2016.
[52] A. L. Rosenbloom, J. R. Joe, R. S. Young, and W. E. Winter, “Emerging

epidemic of type 2 diabetes in youth," *Diabetes Care*, vol. 22, no. 2, pp. 345–354, 1999.

[53] T. A. Hilier and K. L. Pedula, "Complications in Young Adults With Early-Onset Type 2 Diabetes," *Diabetes Care*, vol. 26, no. 11, pp. 2999–3005, 2003.

[54] A. V. Matveyenko and P. C. Butler, "Beta-cell deficit due to increased apoptosis in the human islet amyloid polypeptide transgenic (HIP) rat recapitulates the metabolic defects present in type 2 diabetes," *Diabetes*, vol. 55, no. 7, pp. 2106–2114, 2006.

[55] W. T. Cefalu, "Animal models of type 2 diabetes: clinical presentation and pathophysiological relevance to the human condition.," *ILAR J.*, vol. 47, no. 3, pp. 186–98, 2006.

[56] D. A. Rees and J. C. Alcolado, "Animal models of diabetes mellitus.," *Diabet. Med.*, vol. 22, no. 4, pp. 359–70, 2005.

[57] K. Srinivasan and P. Ramarao, "Animal models in type 2 diabetes research: an overview.," *Indian J. Med. Res.*, vol. 125, no. 3, pp. 451–472, 2007.

[58] A. J. F. King, "The use of animal models in diabetes research," *Br. J. Pharmacol.*, vol. 166, no. 3, pp. 877–894, 2012.

[59] R. Caccetta and H. Al Salami, "Screening for antidiabetic activities," in *Metabolomics Tools for Natural Product Discovery*, 2013, pp. 207–218.

[60] J. Janson *et al.*, "Spontaneous diabetes mellitus in transgenic mice expressing human islet amyloid polypeptide.," *Proc. Natl. Acad. Sci. U. S. A.*, vol. 93, no. July, pp. 7283–7288, 1996.

[61] E. J. P. de Koning *et al.*, "Human islet amyloid polypeptide (IAPP) accumulates at similar sites in islets of transgenic mice and humans," *Diabetes*, vol. 43, no. May, pp. 640–644, 1994.

[62] M. Couce *et al.*, "Treatment with growth hormone and dexamethasone in mice transgenic for human islet amyloid polypeptide causes islet amyloidosis and beta-cell dysfunction.," *Diabetes*, vol. 45, no. 8, pp. 1094–1101, 1996.

[63] R. L. Hull *et al.*, "Increased dietary fat promotes islet amyloid formation and beta-cell secretory dysfunction in a transgenic mouse model of islet amyloid.," *Diabetes*, vol. 52, no. 2, pp. 372–379, 2003.

[64] W. C. Soeller *et al.*, "Islet Amyloid–Associated Diabetes in Obese Avy/a Mice Expressing Human Islet Amyloid Polypeptide," *Diabetes*, vol. 47, no. 17, pp. 743–750.

[65] J. W. M. Höppener *et al.*, "Extensive islet amyloid formation is induced by development of Type II diabetes mellitus and contributes to its progression: Pathogenesis of diabetes in a mouse model," *Diabetologia*, vol. 42, no. 4, pp. 427–434, 1999.

[66] A. E. Butler, J. Jang, T. Gurlo, M. D. Carty, W. C. Soeller, and P. C. Butler, "Diabetes Due to a Progressive Defect in β-Cell Mass in Rats Transgenic for Human Islet Amyloid Polypeptide," *Diabetes*, vol. 53, pp. 1509–1516, 2004.

[67] S. E. Inzucchi *et al.*, "Management of Hyperglycemia in Type 2 Diabetes, 2015: A Patient-Centered Approach: Update to a position statement of the american diabetes association and the european association for the study of diabetes," *Diabetes Care*, vol. 38, no. 1, pp. 140–149, 2015.

[68] A. Lorenzo and B. A. Yankner, "Beta-amyloid neurotoxicity requires fibril formation and is inhibited by congo red.," *Proc. Natl. Acad. Sci. U. S. A.*, vol. 91, no. 25, pp. 12243–7, 1994.

[69] J. F. Aitken, K. M. Loomes, B. Konarkowska, and G. J. S. Cooper, "Suppression by polycyclic compounds of the conversion of human amylin into insoluble

amyloid.," *Biochem. J.*, vol. 374, no. Pt 3, pp. 779–84, 2003.
[70] T. Tomiyama, H. Kaneko, K. I. Kataoka, S. Asano, and N. Endo, "Rifampicin inhibits the toxicity of pre-aggregated amyloid peptides by binding to peptide fibrils and preventing amyloid-cell interaction.," *Biochem. J.*, vol. 322 (Pt 3, pp. 859–65, 1997.
[71] J. J. Meier *et al.*, "Inhibition of human IAPP fibril formation does not prevent β-cell death: evidence for distinct actions of oligomers and fibrils of human IAPP.," *Am. J. Physiol. Endocrinol. Metab.*, vol. 291, no. 6, pp. E1317-24, 2006.
[72] L. A. Scrocchi *et al.*, "Design of peptide-based inhibitors of human islet amyloid polypeptide fibrillogenesis," *J. Mol. Biol.*, vol. 318, no. 3, pp. 697–706, 2002.
[73] L. A. Scrocchi *et al.*, "Inhibitors of islet amyloid polypeptide fibrillogenesis , and the treatment o f type-2 diabetes," *Lett. Pept. Sci.*, vol. 10, pp. 545–551, 2004.
[74] E. T. Jaikaran *et al.*, "Identification of a novel human islet amyloid polypeptide beta-sheet domain and factors influencing fibrillogenesis.," *J. Mol. Biol.*, vol. 308, no. 3, pp. 515–25, 2001.
[75] K. J. Potter *et al.*, "Amyloid inhibitors enhance survival of cultured human islets," *Biochim. Biophys. Acta - Gen. Subj.*, vol. 1790, no. 6, pp. 566–574, 2009.
[76] N. Wijesekara *et al.*, "Islet amyloid inhibitors improve glucose homeostasis in a transgenic mouse model of type 2 diabetes.," *Diabetes Obes Metab*, vol. 17, no. 10, pp. 1003–1006, 2015.
[77] A. Kapurniotu, A. Schmauder, and K. Tenidis, "Structure-based design and study of non-amyloidogenic, double N-methylated IAPP amyloid core sequences as inhibitors of IAPP amyloid formation and cytotoxicity.," *J. Mol. Biol.*, vol. 315, no. 3, pp. 339–350, 2002.
[78] M. Tatarek-Nossol, L. M. Yan, A. Schmauder, K. Tenidis, G. Westermark, and A. Kapurniotu, "Inhibition of hIAPP amyloid-fibril formation and apoptotic cell death by a designed hIAPP amyloid-core-containing hexapeptide," *Chem. Biol.*, vol. 12, no. 7, pp. 797–809, 2005.
[79] L.-M. Yan *et al.*, "Design of a mimic of nonamyloidogenic and bioactive human islet amyloid polypeptide (IAPP) as nanomolar affinity inhibitor of IAPP cytotoxic fibrillogenesis.," *Proc. Natl. Acad. Sci. U. S. A.*, vol. 103, no. 7, pp. 2046–2051, 2006.
[80] L. M. Yan *et al.*, "Selectively N-methylated soluble IAPP mimics as potent IAPP receptor agonists and nanomolar inhibitors of cytotoxic self-assembly of both IAPP and A-beta40," *Angew. Chemie - Int. Ed.*, vol. 52, no. 39, pp. 10378–10383, 2013.
[81] A. Abedini, F. Meng, and D. P. Raleigh, "A single-point mutation converts the highly amyloidogenic human islet amyloid polypeptide into a potent fibrillization inhibitor," *Am. Chem. Soc.*, vol. 129, pp. 11300–1, 2007.
[82] L. Wang, L. Lei, Y. Li, L. Wang, and F. Li, "A hIAPP-derived all-d-amino-acid inhibits hIAPP fibrillation efficiently at membrane surface by targeting α-helical oligomeric intermediates," *FEBS Lett.*, vol. 588, no. 6, pp. 884–891, 2014.
[83] A. Mishra *et al.*, "Conformationally restricted short peptides inhibit human islet amyloid polypeptide (hIAPP) fibrillization.," *Chem. Commun. (Camb).*, vol. 49, no. 26, pp. 2688–90, 2013.
[84] Y. Bram *et al.*, "Apoptosis induced by islet amyloid polypeptide soluble oligomers is neutralized by diabetes-associated specific antibodies," *Sci. Rep.*, vol. 4, no. Dm, p. 4267, 2014.
[85] F. Meng, A. Abedini, A. Plesner, C. B. Verchere, and D. P. Raleigh, "The Flavanol (-)-epigallocatechin 3-gallate inhibits amyloid formation by islet

amyloid polypeptide, disaggregates amyloid fibrils, and protects cultured cells against IAPP-induced toxicity," *Biochemistry*, vol. 49, no. 37, pp. 8127–8133, 2010.

[86] P. Cao and D. P. Raleigh, "Analysis of the inhibition and remodeling of islet amyloid polypeptide amyloid fibers by flavanols," *Biochemistry*, vol. 51, no. 13, pp. 2670–2683, 2012.

[87] H. Noor, P. Cao, and D. P. Raleigh, "Morin hydrate inhibits amyloid formation by islet amyloid polypeptide and disaggregates amyloid fibers," *Protein Sci.*, vol. 21, no. 3, pp. 373–382, 2012.

[88] L. Rivillas-Acevedo, C. Sanchez-Lopez, C. Amero, and L. Quintanar, "Structural basis for the inhibition of truncated islet amyloid polypeptide aggregation by Cu(II): Insights into the bioinorganic chemistry of type II diabetes," *Inorg. Chem.*, vol. 54, no. 8, pp. 3788–3796, 2015.

[89] E. N. Gurzov *et al.*, "Inhibition of hIAPP Amyloid Aggregation and Pancreatic beta-Cell Toxicity by OH-Terminated PAMAM Dendrimer," *Small*, vol. 12, no. 12, pp. 1615–1626, 2016.

[90] P. C. Rosas *et al.*, "Hsp72 (HSPA1A) prevents human islet amyloid polypeptide aggregation and Toxicity: A new approach for type 2 diabetes treatment," *PLoS One*, vol. 11, no. 3, 2016.

[91] M. Ankarcrona *et al.*, "Current and future treatment of amyloid diseases," *J. Intern. Med.*, vol. 280, no. 2, pp. 177–202, 2016.

[92] J. Godyn, J. Jonczyk, D. Panek, and B. Malawska, "Therapeutic strategies for Alzheimer's disease in clinical trials," *Pharmacol. Reports*, vol. 68, no. 1, pp. 127–138, 2016.

[93] J. Sevigny *et al.*, "The antibody aducanumab reduces Aβ plaques in Alzheimer's disease," *Nat. Publ. Gr.*, vol. 537, no. 7618, pp. 50–56, 2016.

[94] R. S. Doody *et al.*, "Phase 3 trials of solanezumab for mild-to-moderate Alzheimer's disease.," *N. Engl. J. Med.*, vol. 370, no. 4, pp. 311–21, 2014.

[95] C. C. Lee *et al.*, "Design and optimization of anti-amyloid domain antibodies specific for beta-amyloid and islet amyloid polypeptide," *J. Biol. Chem.*, vol. 291, no. 6, pp. 2858–2873, 2016.

[96] P. K. Krishnamurthy *et al.*, "Sex and Immunogen-Specific Benefits of Immunotherapy Targeting Islet Amyloid Polypeptide in Transgenic and Wild-Type Mice," *Front. Endocrinol. (Lausanne).*, vol. 7, no. June, pp. 1–15, 2016.

[97] A. Durrer, "In vivo efficacy of human-derived anti-amylin antibodies in a transgenic mouse model of diabetes mellitus," University of Zurich, 2015.

[98] M. Osto, "In vivo efficacy of human-derived anti-human islet amyloid polypeptide antibodies in transgenic rodent models of type 2 diabetes," *Swiss Winter Conf. Ingestive Behav. St. Moritz*, 2014.

[99] M. Osto, "Human-derived antibody targeting pancreatic islet amyloid for the treatment of type 2 diabetes, " *Swiss Winter Conf. Ingestive Behav. St. Moritz*, 2015.

[100] S. Schroeter *et al.*, "Immunotherapy Reduces Vascular Amyloid-beta in PDAPP Mice," *J. Neurosci.*, vol. 28, no. 27, pp. 6787–6793, 2008.

[101] S. Salloway *et al.*, "Two phase 3 trials of bapineuzumab in mild-to-moderate Alzheimer's disease.," *N. Engl. J. Med.*, vol. 370, no. 4, pp. 322–33, 2014.

[102] R. S. Black *et al.*, "A Single Ascending Dose Study of Bapineuzumab in Patients with Alzheimer Disease," *Alzheimer Dis Assoc Disord.*, vol. 24, no. 2, pp. 198–203, 2010.

[103] S. Salloway, S. Gilman, and E. Liu, "A phase 2 multiple ascending dose trial of

bapineuzumab in mild to moderate Alzheimer disease.," *Neurology*, vol. 73, no. September, pp. 2061–2070, 2009.

[104] J. O. Rinne *et al.*, "11C-PiB PET assessment of change in fibrillar amyloid-beta load in patients with Alzheimer's disease treated with bapineuzumab: a phase 2, double-blind, placebo-controlled, ascending-dose study," *Lancet Neurol.*, vol. 9, no. 4, pp. 363–372, 2010.

9 Figures and Tables

9.1 Figures

9.2 Tables

10 Acknowledgement

I would like to thank everyone who supported me and helped me conduct the experiments and complete my doctoral thesis.

In particular, my special thanks go to
Thomas Lutz, for giving me the great chance to work at the Institute of Veterinary Physiology as a doctoral student and for all the help and support during my thesis.
Melania Osto, for the supervision, for supporting me and trusting me during the entire thesis.
Christine Seeger, for her wonderful help and company while performing all the experiments.
Lynda Whiting, for helping me with all the "little things" in the lab.
Fabrice Heitz, for his supportive help while I analyzed the data and prepared my presentation.
Eric Zini, for his helpful and great engagement as co-examiner.
Many thanks to everyone else from our group for the great atmosphere and the support while I was working at the Institute of Veterinary Physiology.

This work was funded by the Commission for Technology and Innovation (CTI).

11 Curriculum Vitae

Vorname Name	Leoni Hugentobler
Geburtsdatum	29/09/1987
Geburtsort	Baden
Nationalität	Schweizerin
Heimatort	Uzwil, SG
08/2003 – 06/2007	Kantonsschule Wettingen (Wettingen, Schweiz)
30/06/2007	Matura (Kantonsschule Wettingen, Wettingen, Schweiz)
09/2007 – 09/2014	Veterinärmedizin Studium (Vetsuisse Fakultät, Zürich, Schweiz)
31/12/2014	Abschlussprüfung vet. med. (Vetsuisse Fakultät, Zürich, Schweiz)
08/2015 – 02/2017	Anfertigung der Dissertation unter Leitung von Prof. Dr. Thomas Lutz am Institut für Veterinärphysiologie, Vetsuisse Fakultät, Zürich, Schweiz Direktor: Prof. Dr. Max Gassmann